A Dual Sampling Communication Method in Wireless Networks

by

Fenyu Jiang

Submitted in partial fulfillment of the requirements of the degree of Doctor of Philosophy

Department of Electronic Engineering and Computer Science
Queen Mary University of London
United Kingdom

January 2020

Statement of Originality

I, Fenyu Jiang, confirm that the research included within this thesis is my own work or that where it has been carried out in collaboration with, or supported by others, that this is duly acknowledged below and my contribution indicated. Previously published material is also acknowledged below.

I attest that I have exercised reasonable care to ensure that the work is original, and does not to the best of my knowledge break any UK law, infringe any third partys copyright or other Intellectual Property Right, or contain any confidential material.

I accept that the College has the right to use plagiarism detection software to check the electronic version of the thesis.

I confirm that this thesis has not been previously submitted for the award of a degree by this or any other university.

The copyright of this thesis rests with the author and no quotation from it or information derived from it may be published without the prior written consent of the author.

Signature:

Date:

Details of collaboration and publications:

- F. Jiang, Y. Sun and C. Phillips, "A Dual Sampling Cooperative Communication Method for Energy and Delay Reduction," 2018 IEEE 16th Intl Conf on Pervasive Intelligence and Computing (PiCom), Athens, 2018, pp. 822-827.
- F. Jiang, Y. Sun and C. Phillips, "Cache Migration Protocol for Information-Centric Networks," 2019 IEEE Wireless Communications and Networking Conference

Workshop (WCNCW), Marrakech, Morocco, 2019, pp. 1-6.

Abstract

As mobile wireless data traffic is increasing significantly, the development direction for wireless networks is focusing on very high data rates, extremely low latency, with a large number of connected devices and a reduction in energy usage. To satisfy the rapid rise in user and traffic capacity, raises challenges given the limited bandwidth resource. The main purpose for this research is to find ways to improve spectral efficiency, data transmission rate, and reduce latency. Simultaneous wireless transmissions happening in the same frequency band can help alleviate demand on transmission slots, with methods like network coding to support decoding at the end terminals. However, in general, signal asynchrony harms the transmission performance significantly. The main contribution of this research is the proposal of a Dual Sampling (DS) method, which aims to relieve the impact of signal asynchrony on simultaneous transmissions. The key concept behind the DS method is sampling twice within each symbol period to handle overlapping signals for successful decoding. Simulation results confirm that it manages to support simultaneous transmissions. Moreover, the DS method is implemented in both Information-Centric Networks (ICN) and Unmanned Aerial Vehicles (UAVs) aided wireless networks. Additionally, for ICN, a Cache Migration Protocol (CMP) is proposed to support simultaneous transmissions which reduces the transmission latency. While for UAV-aided wireless networks, by exploiting the DS method, simultaneous transmissions are supported resulting in better optimal max-min throughput along supported by suitable UAV flight trajectory planning. By demonstrating the performance gain in the application scenarios of ICN and UAV-aided wireless networks, the DS method can be regarded as an optional promising transmission mechanism when communicating with multiple users simultaneously.

Acknowledgments

Firstly, I would like to express my sincere gratitude to my supervisors Dr. Chris Phillips, Dr. Yan Sun and my independent assessor Dr. Miles Hansard for the continuous support of my PhD study and related research, for their patience, motivation, and immense knowledge. Their guidance helped me in all the time of research and writing of this thesis. I could not have imagined having better supervisors for my PhD study.

My sincere thanks also goes to Dr. Yuhang Dai, Dr. Yuhui Yao, and Dr. Liumeng Song, for their suggestions and support to my PhD study.

Last but not the least, I would like to thank my family: my parents, my parents-in-law, my wife, and my son, for supporting me spiritually throughout writing this thesis and my life in general. Especially for my wife Qimeng Guo, without her support and help I could not complete this thesis.

Table of Contents

List of Figures

List of Tables

List of Abbreviations

5G	Fifth Generation
AF	Amplify-and-Forward
AWGN	Additive White Gaussian Noise
BCD	Block Coordinate Descent
BPSK	Binary Phase Shift Keying
BS	Base Station
CMP	Cache Migration Protocol
CS	Content Store
D2D	Device to Device
DF	Decode-and-Forward
DS	Dual Sampling
DTN	Delay Tolerant Networking
FIB	Forwarding Information Base
ICN	Information-Centric Networks
IoT	Internet of Things
LoS	Line-of-Sight
M2M	Machine to Machine
MANET	Mobile Ad hoc NETworks
NDN	Named Data Networking

PIT	Pending Interest Table
QoS	Quality of Service
RWP	Random WayPoint
SCA	Successive Convex Approximation
SI	Self-Interference
SNR	Signal-to-Noise Ratio
UAV	Unmanned Aerial Vehicles
VANET	Vehicular Ad-hoc NETworks
VR	Virtual Reality

Chapter 1

Introduction

With the rapid development of mobile communication technology, communication speed, quality of service and other key mobile communication system metrics have been significantly improved [1] [2] [3]. The performance of mobile terminal equipment improves dramatically, while the cost of it decreases. More and more people choose portable mobile devices to connect with the Internet, which also leads to the number of mobile devices growing rapidly. Receiving network data through mobile devices is becoming the norm for most users, resulting in a dramatic growth of the data traffic in wireless networks. This presents a challenge given the limited wireless transmission resource.

The concept of multicast is widely used nowadays in a wireless environment [4] [5] [6]. Multicast is a routing scheme that transfers copies of a given message to multiple destinations simultaneously. Wireless multicast utilizes the natural broadcasting characteristics of the medium when sending data to reduce unnecessary packet duplication. This enhances the efficiency of data delivery, in other words, reducing the use of transmission resources.

Most data transmission still uses traditional store-and-forward mode [7]. Another transmission mechanism, called network coding, is very different. However, store-and-forward and network coding may be combined, as they are not mutually exclusive.

Network coding integrates different data streams by encoding in relay nodes, and uses a specific method to decode at the destination node(s) to achieve a recovery of each source of data. From the perspective of data forwarding, this mechanism reduces the occupancy of the spectrum. If one uses network coding with wireless multicast as the transmission mechanism, it will typically consume less spectrum resource to transmit a given quantity of information to reach multiple recipients. Currently the variant of network coding with the most promising performance is physical layer network coding.

Physical layer network coding allows multiple wireless transmissions from different nodes via the same bandwidth simultaneously. However, the most challenging issue is signal asynchrony during the transmission. Synchronised signals from the source nodes is essential for the relay node to generate the output without processing errors. If not handled properly, the asynchrony between the source nodes can cause a significant performance penalty in a single channel situation [8]. The results in [9] show that the Signal-to-Noise Ratio (SNR) penalty due to worst case symbol misalignment (half a symbol duration) is about 3dB in an Additive White Gaussian Noise (AWGN) channel. The wireless environment itself has complex characteristics, such as differing and possibly time varying path-lengths between communication endpoints as well as the risk of multi-path signal delivery. So in practice, the signals are often not truly synchronised.

1.1 Motivation

The development trend for wireless networks are to provide higher data rates, enhance end user quality of experience, reduce end-to-end latency, and lower energy consumption [10], with the ultimate aim of larger bandwidth and less latency [11]. It is eagerly been expecting that the wireless network not only enhances the data transfer speed but also energy efficiency, flexibility and good connectivity. It is very important for wireless networks to satisfy the high demand on real time traffic, so that users will experience smooth connectivity to the network [12]. However, a major problem is the interference

during co-channel transmission [13]. Frequency reuse, successive interference cancellation techniques and coordinated multipoint transmissions are some of the popular interference cancellation schemes for mobile wireless networks.

Inspired by the physical layer network coding, some transmitting signal can be treated as useful information rather than interference. The idea of allowing different wireless transmissions to use the same bandwidth during one time slot can efficiently enhance the data transmission procedure both in terms of bandwidth efficiency and less latency. However, how to deal with the signals asynchrony during the simultaneous transmissions remains a challenging issue.

In this research, I found a method to alleviate the impact of signal asynchrony during the simultaneous transmissions, so that to ensure the transmission efficiency. The proposed method extends the applicability of simultaneous transmissions, and can be regarded as an optional promising wireless multiple transmission technique. The proposed method is then involved in some application scenarios leading to less end-to-end latency and larger throughput.

1.2 Research Contributions

As shown in Figure 1.1, my whole research work consists of three parts. The first part is Dual Sampling (DS), the communication method proposed, which is the fundamental of the research work. For the first part, my contributions are:

- Apply cooperative communication to save energy at the relay node;
- Mathematical analysis to estimate the number of cooperative communication structures constructed in a given scenario;
- Propose a DS method to effectively exploit the transmission slots in two-way communications;

My Research Work

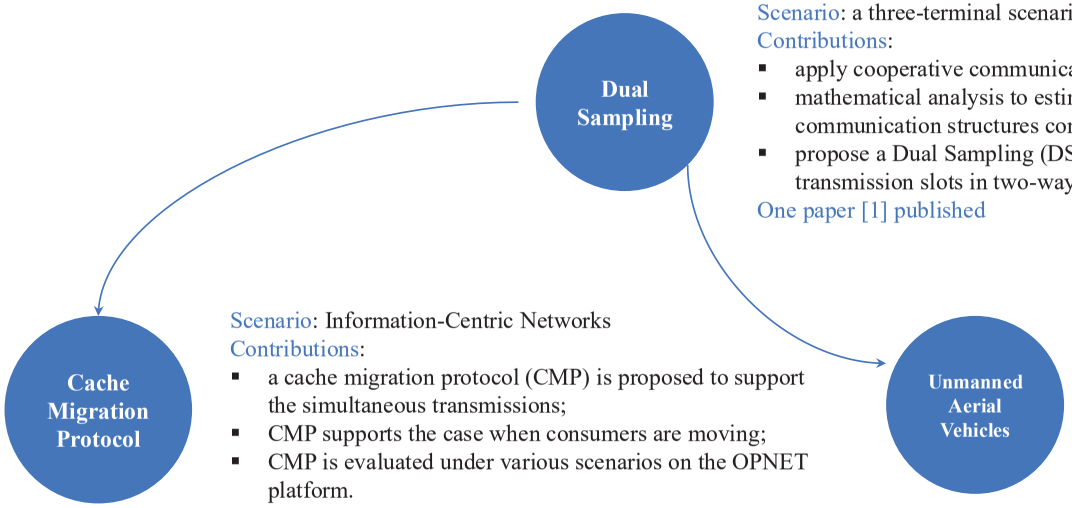

Figure 1.1: Summary of research contribution

[1] F. Jiang, Y. Sun and C. Phillips, "A Dual Sampling Cooperative Communication Method for Energy and Delay Reduction," 2018 IEEE 16th Intl Conf on Pervasive Intelligence and Computing (PiCom), Athens, 2018, pp. 822-827.

[2] F. Jiang, Y. Sun and C. Phillips, "Cache Migration Protocol for Information Centric Networks," 2019 IEEE Wireless Communications and Networking Conference, 2nd Workshop on Intelligent Computing and Caching at the Network Edge, Marrakech, 2019.

- One paper [14] published.

In the second part I propose a Cache Migration Protocol (CMP) to support the DS method in Information-Centric Networks (ICN). The contributions for part two are:

- Propose CMP to support simultaneous transmissions based on DS method;
- CMP supports the case when consumers are moving;
- CMP is evaluated under various scenarios on the OPNET platform;
- One paper [15] published.

For the third part, I try to optimize the transmission throughput of ground terminal in a UAV-aided wireless network on the basis of DS method. The contributions for part three are:

- Propose an iterative algorithm which alternately optimizes bandwidth scheduling and UAV flight trajectory in each iteration, and a power balance method for support DS;
- Comparison of the system performance of a DS-enabled scheme and non-DS schemes in terms of the optimal throughput, bandwidth scheduling and UAV trajectory;
- Comparison of the UAV propulsion energy consumption of a DS-enabled scheme and non-DS schemes based on the derived optimal UAV trajectory;
- One paper has been submitted to Computer Networks on Elsevier.

1.3 Thesis Structure

In this section, the structure of the thesis is listed.

Chapter 2 provides some background related to the proposed DS method, as well

as the ICN and UAV-aided wireless networks application scenarios.

Chapter 3 demonstrates some related works to the applications scenarios for ICN and UAV-aided wireless networks.

Chapter 4 introduces the proposed DS communication method which allows simultaneous transmissions from different nodes during the same transmission slots using the same wireless bandwidth.

Chapter 5 extends the DS method for ICN, and introduces the proposed CMP which appropriately selects the particular nodes to form the typical topology structure for supporting the DS method.

Chapter 6 introduces the DS method in a UAV-aided wireless network scenario in order to plan the UAV flight trajectory for maximizing the minimum data throughput relayed by the UAV among all the ground users.

Chapter 7 concludes the thesis.

References

[1] Lu Y. "Industry 4.0: A survey on technologies, applications and open research issues," Journal of Industrial Information Integration, 2017, 6: 1-10.

[2] Agiwal M, Roy A, Saxena N. "Next generation 5G wireless networks: A comprehensive survey," IEEE Communications Surveys & Tutorials, 2016, 18(3): 1617-1655.

[3] Li S, Da Xu L, Zhao S. "5G Internet of Things: A survey," Journal of Industrial Information Integration, 2018, 10: 1-9.

[4] Lavanya P, Reddy V S K, Prasad A M. "Research and survey on multicast routing protocols for MANETs," 2017 Second International Conference on Electrical, Computer and Communication Technologies (ICECCT). IEEE, 2017: 1-4.

[5] Islam S, Muslim N, Atwood J W. "A survey on multicasting in software-defined networking," IEEE Communications Surveys & Tutorials, 2017, 20(1): 355-387.

[6] Ashour O, St-Hilaire M, Kunz T, et al. "A Survey of Applying Reinforcement Learning Techniques to Multicast Routing," 2019 IEEE 10th Annual Ubiquitous Computing, Electronics & Mobile Communication Conference (UEMCON). IEEE, 2019: 1145-1151.

[7] Liu X, Li Z, Yang P, et al. "Information-centric mobile ad hoc networks and content routing: a survey," Ad Hoc Networks, 2017, 58: 255-268.

[8] L. Lu and S. C. Liew, "Asynchronous physical-layer network coding," IEEE Transactions on Wireless Communications, 2012, 11, pp. 819-831.

[9] S. Zhang, S. C. Liew and P. P. Lam, "On the synchronization of physical layer network coding," 2006 IEEE Information Theory Workshop ITW 06 Chengdu, 2006, pp. 404-408.

[10] Y. Benchaabene, N. Boujnah and F. Zarai, "5G Cellular: Survey on Some Challenging Techniques," 2017 18th International Conference on Parallel and Distributed Computing, Applications and Technologies (PDCAT), Taipei, 2017, pp. 348-353.

[11] V. S. Pandi and J. L. Priya, "A survey on 5G mobile technology," 2017 IEEE International Conference on Power, Control, Signals and Instrumentation Engineering (ICPCSI), Chennai, 2017, pp. 1656-1659.

[12] J. G. Andrews et al., "What Will 5G Be?," in IEEE Journal on Selected Areas in Communications, vol. 32, no. 6, pp. 1065-1082, June 2014.

[13] F. Raisa, A. Reza and K. Abdullah, "Advanced inter-cell interference management technologies in 5G wireless Heterogeneous Networks (HetNets)," 2016 IEEE Student Conference on Research and Development (SCOReD), Kuala Lumpur, 2016, pp. 1-4.

[14] F. Jiang, Y. Sun and C. Phillips, "A Dual Sampling Cooperative Communication Method for Energy and Delay Reduction," 2018 IEEE 16th Intl Conf on Pervasive Intelligence and Computing (PiCom), Athens, 2018, pp. 822-827.

[15] F. Jiang, Y. Sun and C. Phillips, "Cache Migration Protocol for Information-Centric Networks," 2019 IEEE Wireless Communications and Networking Conference Work-

shop (WCNCW), Marrakech, Morocco, 2019, pp. 1-6.

Chapter 2

Background

About two billions people throughout the world use networks for browsing the Web, communicating via emails, accessing multimedia content and services, playing online games, and interacting with friends through social networking applications. This causes heavy data traffic and raises the burden on limited bandwidth resources. While more and more people will gain access to the global information and communication infrastructure, another use of the network is allowing connected machines and smart objects to communicate, compute and coordinate, forming an interconnected clusters of smart objects [1]. The term Internet of Things (IoT) is used to refer to the network of interconnected smart objects that is achieved by means of extended technologies. IoT is an important concept in 5G systems, while D2D and M2M communications are key techniques which can improve the transmission efficiency over many connected users. A large number of applications are built based on IoT concepts, including telecommunications, medical and healthcare, logistics and supply chain management, automotive and transportation [2]. Within these applications, smart objects are mostly connected via wireless channels. Meanwhile, in the wireless environment, smart objects can be transmitters, receivers or relays depending on the functions that are being used.

Low end-to-end transmission delay is a key requirement in nowadays wireless trans-

mission. Without introducing extra cost, it is worthwhile to reduce such delay. In services requiring high Quality of Service (QoS), transmission delay should typically be kept low, in the scale of ms. Applications such as remote control, pilotless vehicles, and industrial automation require low end-to-end transmission latency and high reliability information transmission. For dissemination of real-time videos, with the development of 4K/8K HD techniques, VR (Virtual Reality) interactions, online games and live streams, the definition of the videos is regarded as an important factor. To meet the requirement of high quality images, thresholds are set regarding the transmission delay. For instance, the maximum tolerable transmission delay for 4K HD videos is 12-17ms [3], and for VR applications it is 7ms [4]. The pervasive video call is kind of a two-way communication, similarly, it also relies on low latency and high throughput transmission. Reducing the delay not only improves the transmit efficiency [1], but also brings better service to customers. Before going into further details, a baseline case, the two-way transmission in a three-terminal scenario is considered.

2.1 Two-Way Communication Three-Terminal Scenario

A three-terminal scenario is shown in Figure 2.1. For each one-way transmission, from node S to node D, or from node D to node S, the direct signal between them cannot be correctly interpreted by each other due to the transmission power constraint. It is relayed at node R instead. In the two-way transmission, node S and node D transmit data to each other. This scenario can be regarded as a video call, where nodes S and D are two users communicating with each other via relay R. Or it can be treated as an ICN scenario, and nodes S and D are fetching contents from each other. Figure 2.2(a) illustrates the widely used four-phase transmission with the numerical value over arrow lines indicating each communication phase. However, a number of researchers are working towards two-phase transmission as shown in Figure 2.2(b).

[1]The term transmission efficiency, refers to the data amount transmitted per unit time and per unit bandwidth.

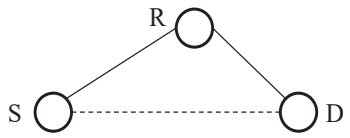

Figure 2.1: A three-terminal scenario

In [5], the authors propose a distributed topology control algorithm to ensure that the final topology is composed of minimum delay paths. Simulations prove that the proposed algorithm can efficiently reduce the network delay. However, this mechanism is based on four-phase transmission. [6] investigates the outage probability of a variable-gain Ampllify-and-Forward (AF) cooperative communication system under two-phase transmission. [7] derives the outage probability of fixed-gain AF cooperative communication. In [8], the Bit-Error-Rate (BER) analysis of hybrid four and two-phase transmissions is presented. A novel two-phase transmission scheme is proposed in [9]. A Decode-and-Forward (DF) cooperative relaying protocol with wireless information and power transfer is investigated in [10]. All of the above works transform four-phase transmissions into two-phase ones. Nevertheless, the methods involve Self-Interference (SI) at the relay, which degrades the system performance. It also costs resources to handle the SI. What's more, the performance of the above methods are affected by the movements of the nodes. In my research work, I creatively find a method which allows different signals to be transmitted simultaneously. Merging different transmissions into one slot provides an efficient approach to reducing network delay. The proposed transmission scheme is shown in Figure 2.2(c).

If the signals asynchrony can be dealt with properly, then there is a method for extracting original information from the overlapped signals via a relay node. For the two-way, three-terminal scenario, information stored in nodes S and D can be used as important components for extracting information. Furthermore, for a more general scenario, as shown in Figure 2.3, assume node S_1 and node S_2 have content A and B, respectively. And assume node D_1 has A_1 and B_1 content parts, while node D_2 has A_2

(a) Four-phase transmission

(b) Existing two-phase transmission

(c) Proposed two-phase transmission

Figure 2.2: Number of transmission phases

and B_2 content parts. To obtain the whole content at nodes D_1 and D_2, simultaneous transmissions can be applied prior to relay forwarding the overlapped signals. Then at nodes D_1 and D_2 we take advantage of network coding [11] to extract the whole content. The case in Figure 2.3 shows that node D_1 obtains content B while node D_2 obtains content A. The above mentioned network coding method is the mechanism used in both later demonstrated ICN and UAV-aided wireless network scenarios, which is the mechanism for decoding information from the overlapped signals in simultaneous transmissions.

The key metric to evaluate a wireless transmission method is BER. In this research, the transmission is assumed to happen in a Rayleigh fading channel with Binary Phase Shift Keying (BPSK), which is a simple example for explanation purposes. In practice there exists more efficient modulation methods. Hence the symbol error rate from a sender to a receiver is [12]

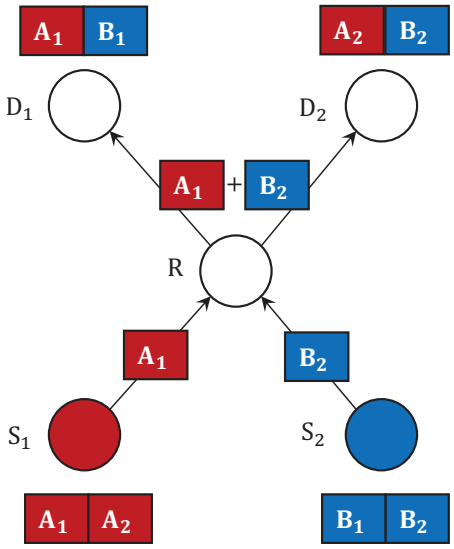

Figure 2.3: Use network coding to extract original information

$$\mathrm{p}(\mathrm{snr}) = \frac{1}{2} - \frac{1}{2}\sqrt{\frac{\mathrm{snr}}{1+\mathrm{snr}}} \tag{2.1}$$

where snr is the average SNR ratio at the receiver.

2.2 Information-Centric Networks

As considered by the International Telecommunication Union [13] [14], acknowledging the heterogeneous service requirements, the architectures like ICN with inherent support for features like name-based networking, in-network storage, edge computing, security, and mobility in 5G are discussed. 5G presents a great opportunity for introducing new network architectures to address service requirements that are difficult to satisfy with current IP networking. A 5G architecture based on ICN can bring benefits on converging computing, storage, and networking over a single platform [15]. As stated in [16], request-to-cache routing is one of the challenges for ICN. In order to take advantage of cached contents, requests have to be forwarded to the nodes that cache

the corresponding contents. However, instructions as to which content is cached where cannot be broadcast throughout the network. Therefore, the knowledge of a content caching location at the time of the request either might not exist or might not be accurate.

Observations of today's Internet behaviour shows that what is being exchanged is becoming more important than where the information is located [17]. The Internet is changing from a communication system to an information exchange platform. The Internet itself is evolving towards the ICN [17], which is considered as a new networking paradigm. It names content in a unique, persistent and location-independent way. The consumer requests its interested content by the corresponding name rather than the storage URL in the Internet. Meanwhile, ICN allows local intra-network caching / replication to take place of the remote content originator. This caching provides a useful approach to reducing the data retrieval latency as well as network congestion. The idea of ICN has been considered in the context of cellular networks with D2D communications to decrease the content retrieval delay [18] [19]. The advantage of ICN in reducing average end-to-end delay in Ad Hoc networks is shown in [20], and the multicast capacity of ICN-enabled Ad Hoc networks is analysed in [21]. Furthermore, leveraging ICN in the IoT is beneficial for improvements in scalability, QoS, content security, energy efficiency and resistance to node mobility [22].

Many researchers focus on the routing issues in the ICN. [23] proposes a routing scheme that is independent of underlying network protocol. It separates the name space from the location space clearly. [24] proposes an ICN-based distributed Resource Directory (RD) architecture. The proposed distributed IoT resource discovery and routing mechanisms allow and reuse existing RD resource registration and lookup interfaces. In [25] the authors proposes a last hop caching protocol in ICN. When the content delivery route is established, the node next to the consumer caches the content for other consumers to request. [26] proposes the Neighbouring Chunk Aware Discovery (NCAD), an active discovery strategy for content routing. NCAD can reduce the

cost of resolving unknown content. NCAD asks the nodes to report back more possession information about the queried content in anticipation of later use. A route discovery mechanism Neighbouring Chunk Aware Flooding (NCAF) is proposed in [27] that makes use of neighbouring chunks to reduce the overhead of successive flooding: when one chunk is requested across the network, its neighbouring chunks are also reported back just in case.

Abundant research achievements about ICN in Mobile Ad hoc NETworks (MANET) is shown in [28]. [29] argues that mobile networks can be made more effective and efficient through Named Data Networking (NDN). Content Centric Networking (CCN) for emergency wireless ad hoc environments is proposed in [30]. The authors extend the CCN architecture by introducing features and requirements especially designed for disruptive networks.

There are some representative routing schemes following the ICN basic principle. Listen First, Broadcast Later (LFBL) [31] chooses the forwarder from a set of eligible nodes based on the shortest distance to the destination principle. Before transmitting the content, each forwarder listens first, if no other nodes sending the same content, it will broadcast the content. Content centric fasHion mANET (CHANET) [32] defers a random time before each transmission to avoid collisions. It also employs a counter-based check during the waiting duration to further reduce the amount of redundant packets. Best Route, Error Broadcast (BREB) [33] preserves a backup routing information from the source to the destination in the potential intermediate nodes. In the case when best route breaks, the destination is able to access the interested content via the backup route. An information-centric architecture for IEEE 802.11 wireless ad hoc networks, named E-CHANET is presented in [34], which performs routing, forwarding and reliable transport functions, specifically tailored to cope with the limitations and requirements of wireless distributed environments.

The work of [35] brings network coding and ICN together at the internetworking layer. It outlines opportunities for applying network coding in a novel and performance-

enhancing way that could push forward the case for ICN itself. [36] addresses the problem of information dissemination in Vehicular Ad-hoc NETworks (VANET) and proposes a model and solution based on a content centric approach of networking and a selective random network coding.

The scenario for applying ICN is first proposed in [37]. [38] provides a guideline to the baseline scenarios in ICN. It states that ICN is inherently suitable for Delay Tolerant Networking (DTN). [39] focuses on a content driven data retrieval model and proposes an enhanced ICN approach based on probability to provide communication resilience to the disruption-prone, delay-tolerant networks. [40] argues that ICN approaches have many benefits for enabling (or continuing) communication after a disaster has impaired a communication network. [41] proposes a communication framework based on messages that exploits Name-based REplication Priorities (NREP) of content and enables ad-hoc communications with spatial and temporal scoping of named messages.

To apply network coding in ICN, the method of learning network topology should be studied. [42] gives an overview of different techniques and algorithms for network topology discovery. [43] discusses a mobile multi-agent-based framework to address the aspect of topology discovery in ad hoc wireless network environment. [44] takes advantage of position error to implement locationing in distributed ad hoc wireless sensor networks. [45] introduces a strategy based on mobile agents and swarm intelligence [46] for topology discovery in an unstructured peer-to-peer networks and wireless ad hoc networks. [47] proposes an IPv6 network topology discovery solution combining the advantages of two discovery methods, based on Internet Control Message Protocol (ICMP) and a routing protocol respectively. In [48], an innovative forwarding strategy, called Density-Aware Directional (DAD), with a joint consideration of vehicle density factor and directional forwarding is proposed for next-hop selection. It is aimed to manage the number of candidate next-hops as function of density and reduce routing loops by involving a directional angle.

2.3 Named Data Networking

NDN is the conventional content delivery scheme for ICN, and the work related to data transmission in ICN should be designed based on NDN. Hence, the NDN forwarding paradigm needs to be reviewed first. The user requesting named content is called the consumer, and it asks for the content by sending an Interest packet indicating its name. There are three main components in NDN forwarding. First, the Forwarding Information Base (FIB) stores the forwarding entries that direct the Interest packets towards the potential source of target content. Second, the Pending Interest Table (PIT) stores the unsatisfied Interest packets and the interfaces on which they were received, so that content can be routed back to the corresponding consumers. Third, the Content Store (CS) is used for caching content. When an Interest packet arrives at a cache router, the CS is checked first for any matching content. If the Interest can be fulfilled by the CS, a Data packet is sent back on the interface on which the Interest packet was received. Otherwise, the content information is looked up through the PIT. If there exists an entry with the same name, the new interface number is added to the interface list, so that a copy of the matching content can be sent on all interfaces from which the Interest packet arrived. Finally, if the Interest packet does not have a matching PIT entry, the Interest packet is forwarded to the next hop based on the FIB.

2.4 Unmanned Aerial Vehicles

Due to the advantages of high mobility and reduced cost, UAVs have been found as promising applications in wireless communication systems [49], not only to support the existing cellular networks in high-demand and overload situations, but also to provide wireless connectivity in scenarios lacking infrastructure such as battlefields or disaster zones. Compared with terrestrial communications, UAV-aided wireless systems are in general faster to deploy, more flexible to reconfigure, and likely to have better communi-

cation channels as a results of Line-of-Sight (LoS) links. The role that a UAV performs in a wireless communication system typically follows either of two types: firstly, the UAV can be deployed as an aerial Base Station (BS) for the ground terminals [50]; secondly, the UAV can be deployed as a mobile relay providing wireless connectivity between distant ground terminals [51] [52]. Especially in disaster scenario there is no terrestrial link between ground terminals, thus the main aim for UAV is to help establish efficient remote communication.

Providing ubiquitous connectivity to diverse device types is the key challenge for 5G and beyond 5G. UAVs are expected to be an important component of the upcoming wireless networks that can potentially facilitate wireless broadcast and support high rate transmissions. Various 5G techniques are introduced on UAV platforms, which are categorized by different domains, including physical layer, network layer, and joint communication, computing and caching [53]. However, energy limitation is the bottleneck in any UAV communications scenario. How to transmit data as much as possible under energy efficiency is a hot research problem.

References

[1] M. H. Asghar, A. Negi and N. Mohammadzadeh, "Principle application and vision in Internet of Things (IoT)," International Conference on Computing, Communication & Automation, Noida, 2015, pp. 427-431.

[2] M. J. Beevi, "A fair survey on Internet of Things (IoT)," 2016 ICETETS, Pudukkottai, 2016, pp. 1-6.

[3] HUAWEI White Paper. [Online]. Available: https://www-file.huawei.com/-/media/corporate/pdf/ilab/smart-wifi-4k-video-transmission-solution-en.pdf

[4] Elbamby M S, Perfecto C, Bennis M, et al. "Toward low-latency and ultra-reliable virtual reality," IEEE Network, 2018, 32(2): 78-84.

[5] Y. Hu, D. Liu and Y. Wu, "A new distributed topology control algorithm based

on optimization of delay in ad hoc networks," 2016 First IEEE International Conference on Computer Communication and the Internet (ICCCI), Wuhan, 2016, pp. 148-152.

[6] D. P. Moya Osorio, et al, "Exploiting the Direct Link in Full-Duplex Amplify-and-Forward Relaying Networks," in IEEE Signal Processing Letters, vol. 22, no. 10, pp. 1766-1770, Oct. 2015.

[7] I. Altunba, A. Ko and A. Yongaolu, "Outage probability of full-duplex fixed-gain AF relaying in Rayleigh fading channels," 2016 Wireless Days (WD), Toulouse, 2016, pp. 1-6.

[8] R. Li, L. Wang, W. Chen, et al, "Bit error rate analysis in hybrid full duplex/half duplex relay cooperative networks," 2016 8th International Conference on Wireless Communications & Signal Processing (WCSP), Yangzhou, 2016, pp. 1-5.

[9] Z. Zhang, et al, "Two-Timeslot Two-Way Full-Duplex Relaying for 5G Wireless Communication Networks," in IEEE Transactions on Communications, vol. 64, no. 7, pp. 2873-2887, July 2016.

[10] Y. Su, L. Jiang and C. He, "Decode-and-forward relaying with fullduplex wireless information and power transfer," in IET Communications, vol. 11, no. 13, pp. 2110-2115, 9 7 2017.

[11] Maddah-Ali M A, Niesen U. "Coding for caching: Fundamental limits and practical challenges," IEEE Communications Magazine, 2016, 54(8): 23-29.

[12] J. G. Proakis, M. Salehi, Digital Communications, 5th ed. New York: McGraw-Hill, 2007.

[13] ITU FG-IMT 2020 Phase-1, "Network Standardization Requirement for 5G," http://www.itu.int/en/ITU-T/focusgroups/imt-2020/ Documents/T13-SG13-151130-TD-PLEN0208!!MSW-E.docx, accessed 02/20/2017.

[14] 5G-Americas: Understanding Information Centric Networking and Mobile Edge Computing, http://www.5gamericas. org/files/3414/8173/2353/ Understanding Information Centric Networking and Mobile Edge Computing.pdf, accessed 02/20/2017.

[15] R. Ravindran, A. Chakraborti, S. O. Amin, A. Azgin and G. Wang, "5G-ICN: Deliv-

ering ICN Services over 5G Using Network Slicing," in IEEE Communications Magazine, vol. 55, no. 5, pp. 101-107, May 2017.

[16] D. Kutscher et al., "RFC 7927:ICN Research Challenges," IRTF, ICNRG, 2016.

[17] V. Jacobson, D. K. Smetters, J. D. Thornton, M. F. Plass, N. H. Briggs, and R. L. Braynard, "Networking named content," in Proc. 5th ACM CoNEXT, 2009.

[18] K. Wang, F. R. Yu and H. Li, "Information-Centric Virtualized Cellular Networks With Device-to-Device Communications," in IEEE Transactions on Vehicular Technology, vol. 65, no. 11, pp. 9319-9329, Nov. 2016.

[19] S. Ullah, T. LeAnh, A. Ndikumana, M. G. R. Alam and C. S. Hong, "Layered video communication in ICN enabled cellular network with D2D communication," 2017 19th Asia-Pacific Network Operations and Management Symposium (APNOMS), Seoul, 2017, pp. 199-204.

[20] R. A. Rehman and B. Kim, "Content Centric Networking Approach in Cognitive Radio Ad Hoc Networks," 2015 13th International Conference on Frontiers of Information Technology (FIT), Islamabad, 2015, pp. 309-313.

[21] G. Zhang, J. Liu and J. Ren, "Multicast capacity of cache enabled content-centric wireless Ad Hoc networks," in China Communications, vol. 14, no. 7, pp. 1-9, July 2017.

[22] M. Amadeo et al., "Information-centric networking for the internet of things: challenges and opportunities," in IEEE Network, vol. 30, no. 2, pp. 92-100, March-April 2016.

[23] Lee J C, Lim W S, Jung H Y. "Scalable domain-based routing scheme for ICN," 2014 International Conference on Information and Communication Technology Convergence (ICTC). IEEE, 2014: 770-774.

[24] Dong L, Ravindran R, Wang G. "ICN based distributed IoT resource discovery and routing," Telecommunications (ICT), 2016 23rd International Conference on. IEEE, 2016: 1-7.

[25] Arifuzzaman M, Keping Y, Nguyen Q N, et al. "Locating the content in the locality: ICN caching and routing strategy revisited," Networks and Communications (EuCNC), 2015 European Conference on. IEEE, 2015: 423-428.

[26] Kai P A N, Hui L I, Weiyang L I U, et al. "Little for More: An Active Discovery Strategy for Content Routing in ICN," China Communications, 13(1z): 54-64.

[27] Chen P, Li D. "NCAF: a reduced flooding mechanism for route discovery in ICN," Communications and Networking in China (CHINACOM), 2014 9th International Conference on. IEEE, 2014: 160-165.

[28] Liu X, Li Z, Yang P, et al. "Information-centric mobile ad hoc networks and content routing: A survey," Ad Hoc Networks, 2016.

[29] Meisel M, Pappas V, Zhang L. "Ad hoc networking via named data. Proceedings of the fifth ACM international workshop on Mobility in the evolving internet architecture," ACM, 2010: 3-8.

[30] Oh S Y, Lau D, Gerla M. "Content centric networking in tactical and emergency manets," Wireless Days (WD), 2010 IFIP. IEEE, 2010: 1-5.

[31] Meisel M, Pappas V, Zhang L. "Listen first, broadcast later: Topologyagnostic forwarding under high dynamics," Annual conference of international technology alliance in network and information science. 2010: 8.

[32] M. Amadeo and A. Molinaro, "CHANET: A content-centric architecture for IEEE 802.11 MANETs," Network of the Future (NOF), 2011 International Conference on the, Paris, 2011, pp. 122-127.

[33] H. Han, M. Wu, Q. Hu and N. Wang, "Best Route, Error Broadcast: A Content-Centric Forwarding Protocol for MANETs," 2014 IEEE 80th Vehicular Technology Conference (VTC2014-Fall), Vancouver, BC, 2014, pp. 1-5.

[34] Amadeo M, Molinaro A, Ruggeri G. "E-CHANET: Routing, forwarding and transport in Information-Centric multihop wireless networks," Computer communications, 2013, 36(7): 792-803.

[35] Montpetit M J, Westphal C, Trossen D. "Network coding meets informationcentric networking: an architectural case for information dispersion through native network coding," Proceedings of the 1st ACM workshop on Emerging Name-Oriented Mobile Networking Design-Architecture, Algorithms, and Applications. ACM, 2012: 31-36.

[36] TalebiFard P, Leung V. "A content centric approach to dissemination of information

in vehicular networks," Proceedings of the second ACM international symposium on Design and analysis of intelligent vehicular networks and applications. ACM, 2012: 17-24.

[37] Trossen D, Sarela M, Sollins K. "Arguments for an information-centric internetworking architecture," ACM SIGCOMM Computer Communication Review, 2010, 40(2): 26-33.

[38] Pentikousis K, Ohlman B, Corujo D, et al. "Information-centric networking: baseline scenarios," 2015.

[39] Monticelli E, Schubert B M, Arumaithurai M, et al. "An information centric approach for communications in disaster situations," 2014 IEEE 20th International Workshop on Local and Metropolitan Area Networks (LANMAN). IEEE, 2014: 1-6.

[40] Seedorf J, Tagami A, Arumaithurai M, et al. "The Benefit of Information Centric Networking for Enabling Communications in Disaster Scenarios," 2015 IEEE Globecom Workshops (GC Wkshps). IEEE, 2015: 1-7.

[41] Psaras I, Saino L, Arumaithurai M, et al. "Name-based replication priorities in disaster cases," Computer Communications Workshops (INFOCOM WKSHPS), 2014 IEEE Conference on. IEEE, 2014: 434-439.

[42] Alhanani R A, Abouchabaka J. "An overview of different techniques and algorithms for network topology discovery," Complex Systems (WCCS), 2014 Second World Conference on. IEEE, 2014: 530-535.

[43] RoyChoudhury R, Bandyopadhyay S, Paul K. "A distributed mechanism for topology discovery in ad hoc wireless networks using mobile agents," Proceedings of the 1st ACM international symposium on Mobile ad hoc networking and computing. IEEE Press, 2000: 145-146.

[44] Chris S, Jan M R, Jail B. "Locationing in Distributed Ad-Hoc wireless sensor network," Proc. of the IEEE International Conference on Acoustics, Speech, and Signal, Salt Lake, USA. 2001: 2037-2040.

[45] Nassu B T, Nanya T, Duarte E P. "Topology discovery in dynamic and decentralized networks with mobile agents and swarm intelligence," Seventh International Conference on Intelligent Systems Design and Applications (ISDA 2007). IEEE,

2007: 685-690.

[46] Dorigo M, Birattari M, Stutzle T. "Ant colony optimization," IEEE computational intelligence magazine, 2006, 1(4): 28-39.

[47] Li M, Yang J, An C, et al. "IPv6 network topology discovery method based on novel graph mapping algorithms," 2013 IEEE Symposium on Computers and Communications (ISCC). IEEE, 2013: 000554-000560.

[48] Hanshi S M, Kadhum M M, Wan T C. "Density-aware directional forwarding strategy for vehicular ad hoc networks," Communications (MICC), 2015 IEEE 12th Malaysia International Conference on. IEEE, 2016: 139-144.

[49] Y. Zeng, R. Zhang, and T. J. Lim, "Wireless communications with unmanned aerial vehicles: Opportunities and challenges," IEEE Commun. Mag., vol. 54, no. 5, pp. 3642, May 2016.

[50] A. Fotouhi et al., "Survey on UAV Cellular Communications: Practical Aspects, Standardization Advancements, Regulation, and Security Challenges," in IEEE Communications Surveys & Tutorials, 2019.

[51] X. Chen, X. Hu, Q. Zhu, W. Zhong and B. Chen, "Channel modeling and performance analysis for UAV relay systems," in China Communications, vol. 15, no. 12, pp. 89-97, Dec. 2018.

[52] Z. Dan, X. Wu, S. Zhu, T. Zhuang and J. Wang, "On the Outage Performance of Dual-Hop UAV Relaying with Multiple Sources," 2019 Cross Strait Quad-Regional Radio Science and Wireless Technology Conference (CSQRWC), Taiyuan, China, 2019, pp. 1-3.

[53] B. Li, Z. Fei and Y. Zhang, "UAV Communications for 5G and Beyond: Recent Advances and Future Trends," in IEEE Internet of Things Journal, vol. 6, no. 2, pp. 2241-2263, April 2019.

Chapter 3

State of the Art

3.1 Dual Sampling Method Related Work

In this section, the research work related to reducing the four-phase to two-phase transmission is first introduced. Then methods to better support simultaneous transmissions, and signal asynchrony handling are discussed.

In-band full-duplex technology allows devices to transmit and receive on the same frequency at the same time. In the two-way communication three-terminal scenario, if a relay node is full-duplex then it can transmit and receive signals during the same time slot, therefore reducing to two-phase communication. However, the potential of full duplex communication can only be realized if the node is equipped with sufficient Self-Interference Cancellation (SIC) techniques [1]. SIC involves the suppression of the transmit signal below certain levels, so as not to cause a large power level difference with the received signal. SIC techniques can be divided into three domains: propagation, analog, and digital, based on the location of where the signal cancellation occurs [1]. For propagation domain techniques, one differs from others mainly in terms of the size, location and direction of the Tx and Rx antennas. The design includes physical separation [2], spatial/beam separation [2], antiphase control [3] [4], circular modes

[5] [6], absorber [7], reflective structures [8] [9], and transmit beamforming [10] [11] [12]. For the analog domain and digital domain SCI techniques, there are time-domain approaches [13], frequency-domain approaches [14] and channel modeling approaches [15]. The function of full-duplex relies on a sufficient number of SIC techniques incorporated, which involve the hardware design of the antenna and signal processing circuits.

There are also other situations that benefit from synchronous transmissions. Low power wireless communication is a central building block of the Internet of Things. Conventional low-power wireless protocols avoid packet collisions by using separated frequencies or time slots. Under specific conditions, low-power wireless radios are often able to receive useful information even in the presence of overlapping signals from different transmitters [16]. The principle of synchronous transmissions is that collisions are not necessarily destructive. By allowing multiple nodes to transmit at the same time on the same carrier frequency, with a high probability a node can receive useful information. Current knowledge indicates that three effects play an important role in whether a node can successfully receive a packet in the presence of collisions: capture effect [17] [18], message-in-message effect [19], and constructive interference [20]. However, synchronous transmissions only work under certain conditions [16]. The key benefits of synchronous transmissions are sender diversity [21], and simplicity by omitting the packet collision avoidance mechanisms. Nevertheless, synchronous transmissions operate on the basis of specific circumstances. And furthermore, it treats weaker signals containing different symbols of information as interference. Thus a simultaneous transmission mechanism that regards signals transmitted by different nodes via same carrier frequency at the same time all as useful information is reasonable, albeit demanding. To analyse the asynchrony of signals in the time domain provides a straightforward view and leads to the evolution of the sampling method.

3.2 Information-Centric Network Related Work

For ICN, the traditional role of local cache memories is to deliver the maximum amount of requested content with reduced delay as well as lessening network traffic. Although this method is optimal for single cache systems, it has been shown to be suboptimal for multiple caches systems [22]. A comparison between caching at the user device for D2D communications and caching at the small cells in cellular networks is discussed in [23]. Nevertheless, the analysis is based on single cache systems. In multiple caches systems, there exists a potential performance gain that can be exploited by merging different transmissions during the content placement stage between the originator and the cache routers. Coded caching [22], which is proposed based on a fundamental understanding of the multiple caches systems, yields a global caching gain [1] by coding the transmission between the originator and the cache routers. Additionally, local delivery gain is possible within the transmissions between cache routers and consumers. Thus far, researchers have focused on finding approaches to achieve global caching gain in various scenarios. Even if a central coordinating server is not available, [24] proposed an efficient decentralized caching scheme which achieves a performance close to the optimal centralized scheme. An efficient algorithm that achieves the gains of coding considering the delay constraints is proposed in [25]. The authors claim that [26] can achieve the optimal rate in which the two layers of cache, in a hierarchical coded caching content delivery network, can simultaneously operate. However, additional delay reduction is possible during the content delivery stage by leveraging a simultaneous transmission mechanism, for instance the DS method [27]. Therefore, a protocol supporting such a transmission technique in multiple caches systems is desirable. So far, a distributed and simultaneous transmission enabled protocol especially for dynamic network context is missing. In my work, a CMP is proposed based on the above statement. After a review of the literature, it is found that no similar protocol is proposed.

[1] The term global caching gain is defined by the authors in [22], which is exploited through coded multicast transmissions from the server that are simultaneously useful for several users, and is different from the local delivery gain available in single cache systems.

Based on the inventory model of Supply Chain Management (SCM) in logistics, a content delivery process of ICN networks is proposed in [28]. The product-centric model of SCM is well suited for the content-centric content delivery process of ICN networks. The proposed scheme operates in a centralized manner, which requires the conditions throughout the network to be collected from the devices, and also consumes time to deal with the content delivery optimization issue. The authors in [29] advocate the need for caching in the Application layer, which can yield a higher cache hit ratio and lower the control and data overhead. This is also a centralized approach.

In [30], a novel wireless ICN architecture Context-Aware Green ICN Model (CAGIM) is proposed. It can adapt the power consumption of nodes according to the corresponding link utilization. The power adaptation is based on adjusting the link-rate related to content popularity and traffic load to reduce wasteful energy consumption. This research is considered within a stable cached-network context, where dynamics due to consumer's joining, leaving and moving are neglected.

[31] presents some common features and compares different architectures that have been proposed for ICN. These architectures generally share the features as name-based service, in-network caching and caching policy. However, they differ in aspects of name-based service, mobility management, content caching and request forwarding. None of these architectures consider exploiting simultaneous transmission techniques to capitalise on the potential performance gains which might be available.

Based on the above analysis, it is found that there are centralized, energy efficient content delivery approaches featuring certain advantages. However, a distributed approach will reduce operational complexity, avoiding the heavy control message flows to and from the central controller, and the ability to support dynamic network context can extend the benefit of the approach. Furthermore, exploiting simultaneous transmissions yields extra performance gains. In Chapter 5, a protocol that jointly considers the above three issues is described, and hence the Cache Migration Protocol is proposed.

CMP is seamless to support the DS method, and intends to migrate the contents to appropriate locations which are easier for fetching, hence a potential solution to the request-to-cache routing challenge in ICN.

3.3 Unmanned Aerial Vehicles Related Work

For Unmanned Aerial Vehicles, how to deploy a UAV in a wireless communication system is a popular research topic [32] [33], as it is related to energy consumption and data transmission performance. There are primarily two categories of UAV deployment studied: static deployment of the UAV [34] [35] [36] and the use of mobile UAVs [37] [38] [39] [40]. The efficient deployment of a UAV acting as a wireless BS providing coverage for ground terminals is analysed in [34] [35]. In [36], the authors propose an intelligent strategy that allows UAVs to perform tactical movements in a disaster scenario, combining the Jaccard distance and algorithms for maximizing the number of served victims. Jaccard distance is a metric to evaluate the difference between two sets, with 0 distance meaning no difference. However, the analysis is based on static deployment of the UAV. The authors in [41] propose a simple but effective dynamic trajectory control algorithm for UAVs. The proposal adjusts the centre coordinates and the radius of UAVs' trajectories in order to alleviate congestion. Nevertheless, the method is implemented by a UAV control station, which introduces control signal overhead.

In regard to mobile UAV deployment, the UAV flight trajectory is planned considering the wireless communication features. A UAV that acts as a mobile BS serving a group of ground terminals to maximize the throughput is demonstrated in [37]. The UAV flies in a cyclical pattern and the ground terminals are located along a straight line, rather than a 2D plane. An energy-efficient data collection problem in UAV-aided wireless sensor network is solved in [38]. The authors only consider one common transmission channel that all the sensors have to contend for using a time division multiple access scheme. The resource allocation and trajectory design for energy-efficient secure

UAV communication system is studied in [39]. The authors consider the ground terminals to transmit data via separate sub-carriers so as to avoid interference. A joint trajectory and communication design for UAV-enabled system is elaborated in [40]. The data transmission in these above-mentioned works are in orthogonal channels, either in different time slots or in different transmission bands. However, simultaneous transmission techniques like the DS method which allow different data signals to be transmitted during the same time slot and radio band have not been considered in the UAV-aided wireless communication systems. By supporting the DS method during UAV transmission, it is expected to improve the system efficiency on improving the average transmission throughput among all the ground terminals.

References

[1] Kolodziej K E, Perry B T, Herd J S, "In-band full-duplex technology: Techniques and systems survey," IEEE Transactions on Microwave Theory and Techniques, 2019, 67(7): 3025-3041.

[2] Everett E, Sahai A, Sabharwal A, "Passive self-interference suppression for full-duplex infrastructure nodes," IEEE Transactions on Wireless Communications, 2014, 13(2): 680-694.

[3] Makar G, Tran N, Karacolak T, "A high-isolation monopole array with ring hybrid feeding structure for in-band full-duplex systems," IEEE Antennas and Wireless Propagation Letters, 2016, 16: 356-359.

[4] Tianang E G, Filipovic D S, "A dipole antenna system for simultaneous transmit and receive," 2015 IEEE International Symposium on Antennas and Propagation & USNC/URSI National Radio Science Meeting. IEEE, 2015: 428-429.

[5] Lian R, Shih T Y, Yin Y, et al, "A high-isolation, ultra-wideband simultaneous transmit and receive antenna with monopole-like radiation characteristics," IEEE Transactions on Antennas and Propagation, 2017, 66(2): 1002-1007.

[6] Etellisi E A, Elmansouri M A, Filipovi D S, "Wideband multimode monostatic spi-

ral antenna STAR subsystem," IEEE Transactions on Antennas and Propagation, 2017, 65(4): 1845-1854.

[7] Cacciola R, Holzman E, Carpenter L, et al, "Impact of transmit interference on receive sensitivity in a bi-static active array system," 2016 IEEE International Symposium on Phased Array Systems and Technology (PAST). IEEE, 2016: 1-5.

[8] Elmansouri M A, Filipovic D S, "Realization of ultra-wideband bistatic simultaneous transmit and receive antenna system," 2016 IEEE International Symposium on Antennas and Propagation (APSURSI). IEEE, 2016: 2115-2116.

[9] Xu H, Zhou H, Gao S, et al, "Multimode decoupling technique with independent tuning characteristic for mobile terminals," IEEE Transactions on Antennas and Propagation, 2017, 65(12): 6739-6751.

[10] Snow T, Fulton C, Chappell W J, "Multi-antenna near field cancellation duplexing for concurrent transmit and receive," 2011 IEEE MTT-S International Microwave Symposium. IEEE, 2011: 1-4.

[11] Everett E, Shepard C, Zhong L, et al, "Softnull: Many-antenna full-duplex wireless via digital beamforming," IEEE Transactions on Wireless Communications, 2016, 15(12): 8077-8092.

[12] Aryafar E, Khojastepour M A, Sundaresan K, et al, "MIDU: Enabling MIMO full duplex," Proceedings of the 18th annual international conference on Mobile computing and networking. 2012: 257-268.

[13] Yang X, Babakhani A, "A single-chip in-band full-duplex low-if transceiver with self-interference cancellation," 2016 IEEE MTT-S International Microwave Symposium (IMS). IEEE, 2016: 1-4.

[14] Krishnaswamy H, Zussman G, Zhou J, et al, "Full-duplex in a hand-held device from fundamental physics to complex integrated circuits, systems and networks: An overview of the columbia flexicon project," 2016 50th Asilomar Conference on Signals, Systems and Computers. IEEE, 2016: 1563-1567.

[15] Adams M, Bhargava V K, "Use of the recursive least squares filter for self interference channel estimation," 2016 IEEE 84th Vehicular Technology Conference (VTC-Fall). IEEE, 2016: 1-4.

[16] Zimmerling M, Mottola L, Santini S, "Synchronous transmissions in low-power wireless: A survey of communication protocols and network services," arXiv preprint arXiv:2001.08557, 2020.

[17] Knig M, Wattenhofer R, "Maintaining constructive interference using well-synchronized sensor nodes," 2016 International Conference on Distributed Computing in Sensor Systems (DCOSS). IEEE, 2016: 206-215.

[18] Liao C H, Katsumata Y, Suzuki M, et al, "Revisiting the so-called constructive interference in concurrent transmission," 2016 IEEE 41st Conference on Local Computer Networks (LCN). IEEE, 2016: 280-288.

[19] Manweiler J, Santhapuri N, Sen S, et al, "Order matters: transmission reordering in wireless networks," IEEE/ACM Transactions on Networking, 2011, 20(2): 353-366.

[20] Ferrari F, Zimmerling M, Thiele L, et al, "Efficient network flooding and time synchronization with glossy," Proceedings of the 10th ACM/IEEE International Conference on Information Processing in Sensor Networks. IEEE, 2011: 73-84.

[21] Tse D, Viswanath P, "Fundamentals of wireless communication," Cambridge university press, 2005.

[22] M. A. Maddah-Ali and U. Niesen, "Coding for caching: fundamental limits and practical challenges," in IEEE Communications Magazine, vol. 54, no. 8, pp. 23-29, August 2016.

[23] Z. Chen and M. Kountouris, "D2D caching vs. small cell caching: Where to cache content in a wireless network?," 2016 IEEE 17th International Workshop on Signal Processing Advances in Wireless Communications (SPAWC), Edinburgh, 2016, pp. 1-6.

[24] M. A. Maddah-Ali and U. Niesen, "Decentralized Coded Caching Attains Order-Optimal Memory-Rate Tradeoff," in IEEE/ACM Transactions on Networking, vol. 23, no. 4, pp. 1029-1040, Aug. 2015.

[25] U. Niesen and M. A. Maddah-Ali, "Coded caching for delay-sensitive content," 2015 IEEE International Conference on Communications (ICC), London, 2015, pp. 5559-5564.

[26] N. Karamchandani, U. Niesen, M. A. Maddah-Ali and S. N. Diggavi, "Hierarchical

Coded Caching," in IEEE Transactions on Information Theory, vol. 62, no. 6, pp. 3212-3229, June 2016.

[27] F. Jiang, Y. Sun and C. Phillips, "A Dual Sampling Cooperative Communication Method for Energy and Delay Reduction," 2018 IEEE 16th Intl Conf on Pervasive Intelligence and Computing (PiCom), Athens, 2018, pp. 822-827.

[28] Z. Feng, M. Xu, Y. Yang, Y. Wang, Q. Li and W. Wang, "Optimizing content delivery in ICN networks by the supply chain model," 2016 IEEE 35th International Performance Computing and Communications Conference (IPCCC), Las Vegas, NV, 2016, pp. 1-8.

[29] J. Chen, H. Xu, S. Penugonde, Y. Zhang and D. Raychaudhuri, "Exploiting ICN for Efficient Content Dissemination in CDNs," 2016 Fourth IEEE Workshop on Hot Topics in Web Systems and Technologies (HotWeb), Washington, DC, 2016, pp. 14-19.

[30] Q. N. Nguyen, M. Arifuzzaman, K. Yu and T. Sato, "A Context-Aware Green Information-Centric Networking Model for Future Wireless Communications," in IEEE Access, vol. 6, pp. 22804-22816, 2018.

[31] Feixiong Zhang, "Comparing alternative approaches for mobile content delivery in information-centric networking," 2015 IEEE 16th International Symposium on A World of Wireless, Mobile and Multimedia Networks (WoWMoM), Boston, MA, 2015, pp. 1-2.

[32] L. Ruan et al., "Energy-efficient multi-UAV coverage deployment in UAV networks: A game-theoretic framework," in China Communications, vol. 15, no. 10, pp. 194-209, Oct. 2018.

[33] X. Zhang and L. Duan, "Fast Deployment of UAV Networks for Optimal Wireless Coverage," in IEEE Transactions on Mobile Computing, vol. 18, no. 3, pp. 588-601, 1 March 2019.

[34] M. Mozaffari, W. Saad, M. Bennis and M. Debbah, "Drone Small Cells in the Clouds: Design, Deployment and Performance Analysis," 2015 IEEE Global Communications Conference (GLOBECOM), San Diego, CA, 2015, pp. 1-6.

[35] M. Mozaffari, W. Saad, M. Bennis and M. Debbah, "Efficient Deployment of Multi-

ple Unmanned Aerial Vehicles for Optimal Wireless Coverage," in IEEE Communications Letters, vol. 20, no. 8, pp. 1647-1650, Aug. 2016.

[36] J. Snchez-Garca, J. M. Garca-Campos, S. L. Toral, D. G. Reina, and F. Barrero. 2016. "An Intelligent Strategy for Tactical Movements of UAVs in Disaster Scenarios," Int. J. Distrib. Sen. Netw. 2016.

[37] J. Lyu, Y. Zeng and R. Zhang, "Cyclical Multiple Access in UAV-Aided Communications: A Throughput-Delay Tradeoff," in IEEE Wireless Communications Letters, vol. 5, no. 6, pp. 600-603, Dec. 2016.

[38] C. Zhan, Y. Zeng and R. Zhang, "Energy-Efficient Data Collection in UAV Enabled Wireless Sensor Network," in IEEE Wireless Communications Letters, vol. 7, no. 3, pp. 328-331, June 2018.

[39] Y. Cai, Z. Wei, R. Li, D. Ng and J. Yuan. "Energy-Efficient Resource Allocation for Secure UAV Communication Systems," in IEEE WCNC Proceedings, 2019.

[40] Q. Wu, Y. Zeng and R. Zhang, "Joint Trajectory and Communication Design for UAV-Enabled Multiple Access," GLOBECOM 2017 - 2017 IEEE Global Communications Conference, Singapore, 2017, pp. 1-6.

[41] Z. M. Fadlullah, D. Takaishi, H. Nishiyama, N. Kato and R. Miura, "A dynamic trajectory control algorithm for improving the communication throughput and delay in UAV-aided networks," in IEEE Network, vol. 30, no. 1, pp. 100-105, January-February 2016.

Chapter 4

Dual Sampling Method

In this chapter, the work starts with a three-terminal scenario. Regarding the two-way transmission, a DS method is proposed to reduce the overall delay. Moreover, different from the Decode-and-Forward (DF) relaying scheme, the approach also takes the signal from the direct link for decoding at the receiver. By deriving the BER expressions, it is observed that under same energy consumption constraint, the proposed approach outperforms DF relaying. Finally, an expression for estimating the number of such three-terminal clusters in a random wireless network is derived. Simulations results confirm that the DS method not only alleviates the average two-way transmission delay, but also saves transmission energy in the three-terminal scenario.

For this chapter, the contributions can be summarized as follows:

- Propose a DS method to effectively exploit the transmission slots in two-way communication. Taking advantage of the characteristics of wireless transmission, the approach naturally allows different signals to overlap when they are transmitted simultaneously. We then apply the proposed DS method to separate the overlapped signals at the receiver. Under the same bandwidth constraint, the delay is decreased because otherwise sequential transmissions can be merged into a single transmission.

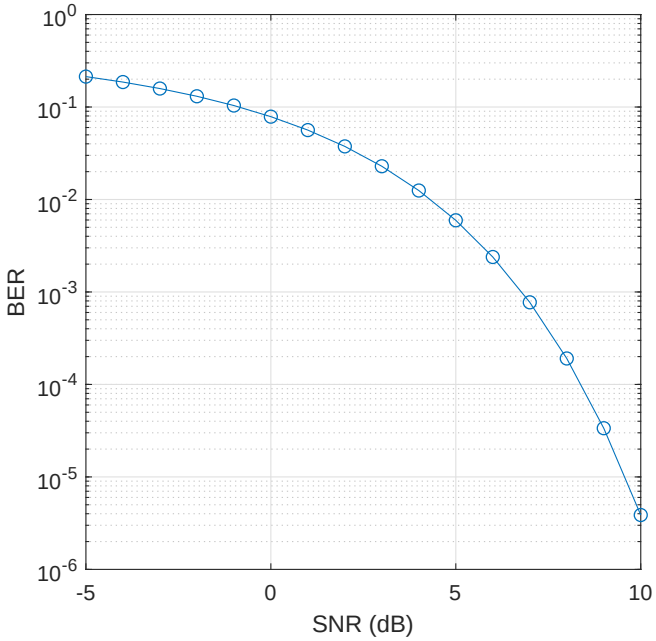

Figure 4.1: BER curve for BPSK

- Apply cooperative communication to save energy at the relay node in a three-terminal scenario. In this chapter, it is proved that under the same BER requirement, the cooperative communication technique consumes less energy at the relay node.

- Perform mathematical analysis to estimate the number of three-terminal structures constructed in a given scenario. This analysis provides an estimate of the potential three-terminal communication within a wireless network topology. On using the derived mathematical expressions it allows the benefit gained by cooperative communication to be estimated without the actual deployment of a real wireless communication system.

Before going into details of the DS method, the BER curve for the BPSK modulation method is shown in Figure 4.1. This corresponds to each phase in the four transmission phases. Thus, the impact caused by signal asynchrony is not considered.

Figure 4.2: DS method transmission

4.1 Dual Sampling

This section elaborates the proposed DS method for two-way transmission in a three-terminal scenario as shown in Figure 4.2. The scenario is two distant nodes communicating with each other via a relay node, such as a video call or content retrieval in ICN. Nodes S and D wish to exchange information. Assume nodes S and D work in full-duplex mode, while node R works in half-duplex mode. In the proposed scheme, both nodes S and D transmit information to R in the first phase. In general, signals from nodes S and D reach R asynchronously. The asynchrony is mainly caused by the imperfect synchronous transmission of nodes S and D. To reduce the impact of the signals asynchrony, node R uses DS to infer the original combined signal based on the received overlapping signals before transmitting to S and D in the second phase. In the first phase, both S and D face Self-Interference (SI) as they transmit and receive information simultaneously. However, S and D can apply DS to deal with the mixed signal to obtain the signal from the other node. Finally, upon receiving the inferred signal from R, both S and D can subtract the original signal from it to extract the information from the other node.

As the transmission from R to nodes S and D is the end-to-end wireless transmission, thus the remaining text focuses on explaining the DS method used at R. S and D take similar actions when dealing with SI based on DS method. For convenience, we express the duration of one symbol as one time unit. Each symbol is carried as a rectangular signal

$$g(t) = u(t+1) - u(t) \tag{4.1}$$

$$u(t) = \begin{cases} 1 & t \geq 0 \\ 0 & t < 0 \end{cases} \tag{4.2}$$

The baseband signal received by R from S is

$$\sum_{n=1}^{N} h_{\mathrm{SR}} x_1[n] g(t-n) \tag{4.3}$$

where $h_{\mathrm{SR}} = \sqrt{P_{\mathrm{S}}}$, P_{S} is the received signal power from node S at relay R. $x_1[n]$ are symbols of S with length N, that is the signal of S consists of N symbols. Similarly, the baseband signal received by R from node D is

$$\sum_{n=1}^{N} h_{\mathrm{DR}} x_2[n] g(t-n) \tag{4.4}$$

where $h_{\mathrm{DR}} = \sqrt{P_{\mathrm{D}}}$, P_{D} is the received signal power from node D at relay R, $x_2[n]$ are node D's symbols with length N. Assume power control is pre-performed such that $\sqrt{P_{\mathrm{S}}} = \sqrt{P_{\mathrm{D}}} = \sqrt{P}$. The mixed signals that R receives can be expressed as:

$$r(t) = \sum_{n=1}^{N} \sqrt{P}\{x_1[n] g(t-n) + \mathrm{e}^{j\phi} x_2[n] g(t-n-\Delta)\} + w(t) \tag{4.5}$$

where ϕ is the relative phase offset and Δ is the symbol misalignment between the two signals, also Δ can be regarded as the relative time difference. $w(t)$ is the AWGN with double-sided spectrum variance $\frac{N_0}{2}$, for both real and imaginary components. At the relay node R, it is possible to infer signals from $r(t)$, and then transmit the inferred

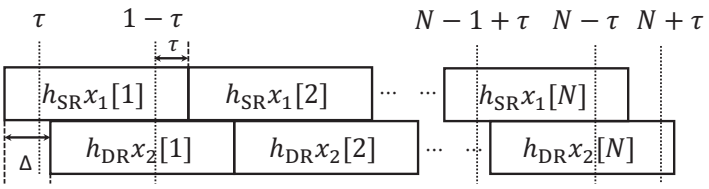

Figure 4.3: DS method within one symbol

synchronized signal to S and D. Finally, S and D receive the inferred signal, and decode the signal by subtracting their own original signal. The DS method is triggered when two different transmissions via the same frequency band are detected by the relay node; otherwise the DS method will not be started. The transmission starts at nodes S and D do not have to be precisely the same. As long as their transmissions overlap to some extent, the DS method is able to operate. If there is no overlap, the DS method is not be triggered.

This method is designed to utilize the unsynchronized incoming signals at relay R. Assume the range of symbol misalignment between S and D is $0 < \Delta < 1$ [1]. Another variable τ is defined to locate the two sampling points within one symbol. Assume that the signal from S arrives R earlier than that from D.

The odd sampling point is τ behind the beginning of a symbol S, in time. The even sampling point is located τ prior to the end of the same S symbol, as shown in Figure 4.3. To sum up, given the signal consists of N symbols, the odd sampling instants are at $n - 1 + \tau$, while the even sampling instants are at $n - \tau$, where $n = 1, 2, \ldots, N$.

At time instants $n - 1 + \tau$ and $n - \tau$, where $n = 1, 2, \ldots, N$, the samples are values out of the matched filter:

[1] $0 < \Delta < 1$ is the worst case where the two signals overlap with each other the most. It is reasonable to analyse this case as when $\Delta > 1$ there would be less error.

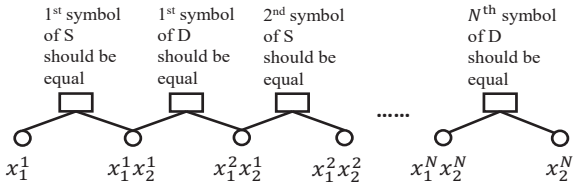

Figure 4.4: Tanner graph for original signal inference

$$\begin{aligned} r[2n-1] &= \frac{1}{\tau}\int_{n-1}^{n-1+\tau} \frac{r(t)}{\sqrt{P}}\mathrm{d}t \\ &= x_1[n] + \mathrm{e}^{j\phi}x_2[n-1] + w[2n-1] \end{aligned} \tag{4.6}$$

$$r[2n] = \frac{1}{\tau}\int_{n-\tau}^{n} \frac{r(t)}{\sqrt{P}}\mathrm{d}t = x_1[n] + \mathrm{e}^{j\phi}x_2[n] + w[2n] \tag{4.7}$$

where $w[2n-1]$ and $w[2n]$ are zero-mean complex Gaussian noises with variance $\frac{N_0}{2P\tau}$ for both real and imaginary components.

In total, $2N+1$ samples will be obtained by the DS method. Assume BPSK is used as the modulation method such that $x_1[n], x_2[n] \in \{+1, -1\}$. It applies the Tanner graph as shown in Figure 4.4 to distinguish the original S and D signals. Use x_1^n, x_2^n to represent the n^{th} symbol of S and D. The detected samples are expressed by $x_1^n x_2^{n-1}$ and $x_1^n x_2^n$ as mixtures of S and D symbols. These detected mixed values are represented as circular observed nodes in Figure 4.4, while the rectangles represent the constraint nodes connecting every two adjacent circular nodes. Based on the observed $2N+1$ samples, the following probabilities can be obtained:

$$\mathrm{p}_{2n-1}^{a,b} = \mathrm{P}(x_1[n] = a, x_2[n-1] = b | r[2n-1]) \tag{4.8}$$

$$\mathrm{p}_{2n}^{a,b} = \mathrm{P}(x_1[n] = a, x_2[n] = b | r[2n]) \tag{4.9}$$

where $a, b \in \{+1, -1\}$. Focus on $\mathrm{p}_{2n}^{a,b}$ as it is directly related to the inference resulting from the combination of the original bits. With the constraint nodes, the $(2n-1)^{\mathrm{th}}$ and $2n^{\mathrm{th}}$ samples should satisfy the condition that the n^{th} symbol from node S are identical. Thus, $\mathrm{p}_{2n}^{a,b}$ can be further written as below:

$$\mathrm{p}_{2n}^{a,b} = \mathrm{p}_{2n}^{a,b} \times \mathrm{p}_{2n-1}^{a} \tag{4.10}$$

$$\mathrm{p}_{2n-1}^{a} = \mathrm{p}_{2n-1}^{a,+1} + \mathrm{p}_{2n-1}^{a,-1} \tag{4.11}$$

With the newly calculated $\mathrm{p}_{2n}^{a,b}$, the combination $x_1[n] = a, x_2[n] = b$ results in the maximum $\mathrm{p}_{2n}^{a,b}$ value that should be selected as the inference. Since the graph contains no loop, it provides complete convergence, which guarantees that all the symbol pairs from S and D can be inferred. It is worth pointing out that the proposed DS method increases the complexity by doubling the sample rate. However, it locates the two sampling points at symmetric positions within one symbol, which is more specific than simply doubling the sample rate.

4.2 Dual Sampling Performance Evaluation

In this section, the performance of the DS method in a two-way three-terminal scenario is evaluated. The DS method can be applied in a real wireless network scenario, for example the wireless sensor networks. We run the same experiment for multiple times to provide confidence intervals, indicating that the results achieved are statistically significant and the degree of variation observed, since the wireless transmissions are a

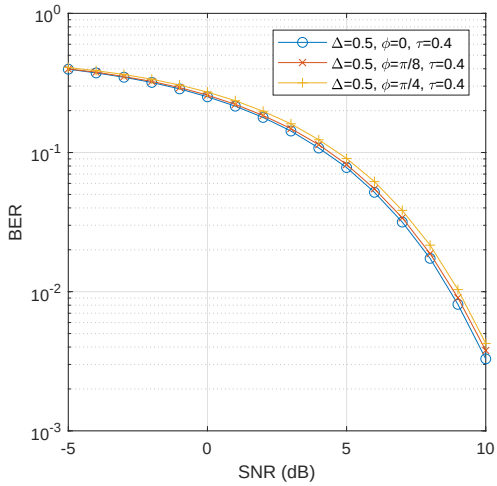

Figure 4.5: DS, $\Delta = 0.5, \tau = 0.4$, change ϕ

form of event that occur is kind of event based on probability. Nodes S and D exchange information via relay R. The simulation is carried out with S and D signals of 500 packets, each packet containing 2048 bits. Note that, $P/N_0 = E_s/N_0$ is the received SNR at R for both S and D signals. In the simulations of the DS method, the range of received SNR is set from -5dB to 10dB.

Figure 4.5 provides the BER performance of DS given Δ =0.5 and τ =0.4 under three values of ϕ $[0, \pi/8, \pi/4]$. As expected, the BER performance improves with increasing the SNR. Nevertheless, the difference in BER performance caused by phase offset is slight.

In Figure 4.6, DS simulations are carried out with Δ =0.5 and $\phi = \pi/4$ under different τ [0.4, 0.3, 0.2]. The corresponding 95% confidence interval for the BER results is shown in Figure 4.7. Assuming Δ is located between the two sampling points, the larger the value of τ, the better is the BER performance that is achieved. For complex Gaussian noise with variance $\frac{N_0}{2P\tau}$, increasing τ leads to a smaller noise power, thus resulting in better BER performance. Furthermore, in Figure 4.14, for each BER curve, the 95% confidence interval upper and lower bounds are almost identical to the average simulation results. Therefore, the simulation results averaged on multiple trials can be

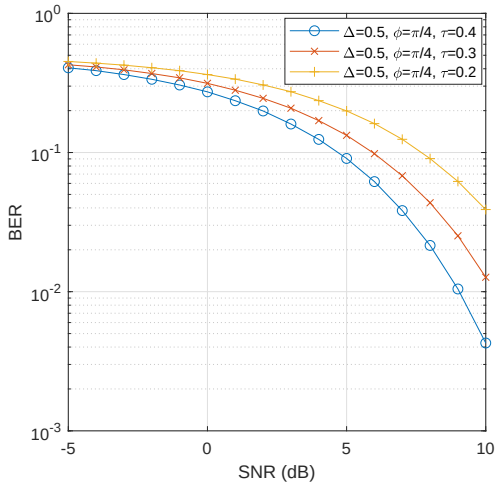

Figure 4.6: DS, $\Delta = 0.5, \phi = \pi/4$, change τ

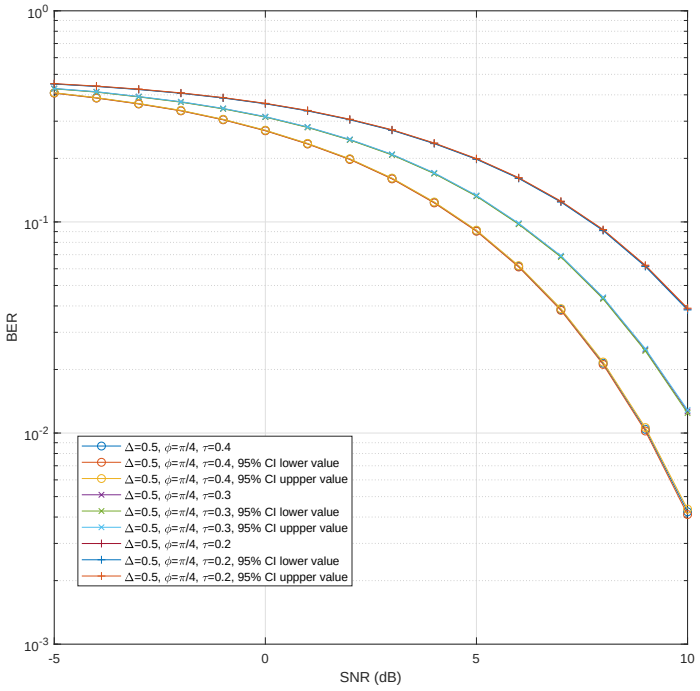

Figure 4.7: DS, $\Delta = 0.5, \phi = \pi/4$, change τ, with 95% confidence interval

trusted as a representative for evaluating the BER performance.

As shown in Figure 4.8, the DS method with $\phi = \pi/4$ and different combinations of Δ and τ is simulated. When Δ =0.1, τ =0.8 and Δ =0.5, τ =0.4, the even samples $r[2n]$

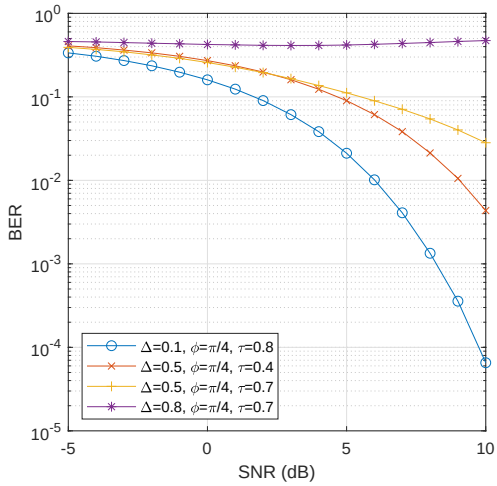

Figure 4.8: DS, $\phi = \pi/4$, change Δ, τ

only contain $x_1[n]$ and $x_2[n]$, which introduce no extra errors to the inference procedure. When Δ =0.5, τ =0.7 and Δ =0.8, τ =0.7, $r[2n]$ contains $x_1[n]$, part of $x_2[n]$ and part of $x_2[n-1]$, which makes the inference results less correct. Furthermore, if $r[2n]$ contains a greater part of $x_2[n-1]$ and a lesser part of $x_2[n]$, more error information would be processed, thus worsening the BER performance. Hence, the even sampling instants mainly affect the DS method performance.

Figure 4.9 provides a performance comparison between transmissions based on the conventional one sampling method and the DS scheme by changing the SNR at R. When $r[2n]$ only contains $x_1[n]$ and $x_2[n]$ for the DS method with the same Δ and ϕ, DS outperforms the one sampling method. In the one sampling method, a greater Δ worsens the BER performance, as larger symbol misalignment introduces more mismatched information into the decoding process.

Next the delay reduction performance of DS method is investigated. Figure 4.10 provides a comparison of the average delay between non-DS and DS method. Consider a two-way transmission scenario. The transmission rate is 1Mb/s and both S and D transmit the same amount of data. By observing the results, DS outperforms non-DS in terms of average delay. When the transmitted data size increases, the average delay for

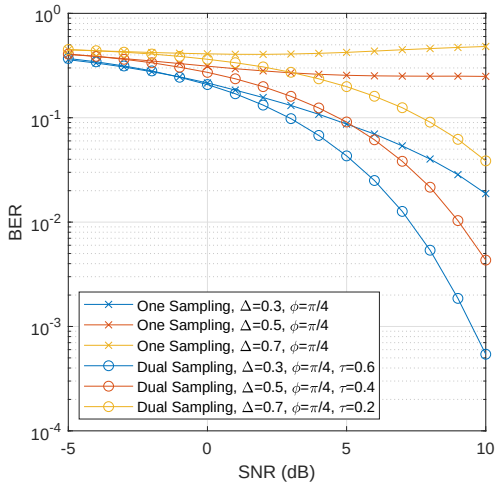

Figure 4.9: Dual sampling vs. one sampling

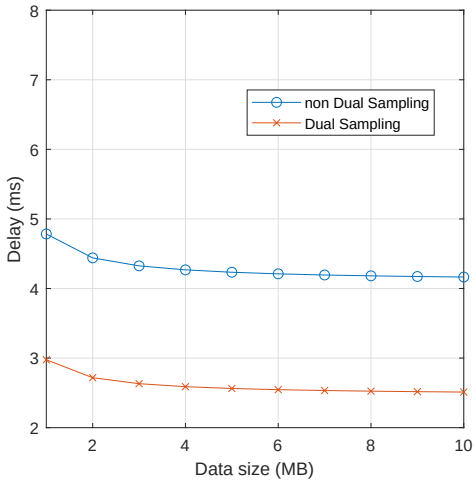

Figure 4.10: Average end-to-end delay comparison

both methods decreases, which is due to reduced handshaking. To be specific, although a set-up procedure is needed for both methods prior to transmitting data, which takes some time, when the transmission data size increases, the negative impact of the set-up procedure is reduced. The results shown in Figure 4.10 are compatible with the latency constraints for wireless transmission in the fields of healthcare, education and gaming [1].

4.3 Dual Sampling with Cooperative Communication

In a wireless environment, smart objects are often energy limited due to their design and hardware constraints. Hence, it is reasonable to develop approaches for saving energy. According to the International Energy Agency, there will be over 14 billion network-enabled devices, compared to approximately 3.2 billion people using the Internet by 2020. It will definitely consume a significant amount of power. The industries and researchers are finding approaches to reduce the power consumption of connected devices in order to save resources. Almost all mobile devices are supplied by batteries. To extend the battery life of sensors, self-sustaining is needed by generating electricity from environmental elements such as vibrations, light, and airflow. Improvements to the transmission mechanism are also possible. A modified adaptive data rate control method is proposed to consume low power for data transmission in long-range IoT services [2]. Cooperative communication has been proposed to enable single-antenna nodes to share their antennas and generate a virtual multiple-antenna that allows them to achieve transmission diversity. With cooperative communication, the baseline transmit power for nodes is reduced through this diversity. The BER performance of both Amplify-and-Forward (AF) and DF cooperative communication are analysed in [3] to realize green communication. The analysis is performed with a three-terminal scenario, and it proves that DF always outperforms AF in terms of BER.

In the baseline scenario, i.e. the two-way communication three-terminal case, for transmission from node S to D, two independent paths exist which provides cooperative communication diversity. Even though the signal power via the direct link from node S to D is weak, it is able to provide extra energy gain combined with the signal via relay R. With the application of cooperative communication, the weak direct signal increases the equivalent SNR for the transmission BER analysis, therefore leads to better overall BER performance.

In this section, BER expressions for both DF relaying and cooperative communi-

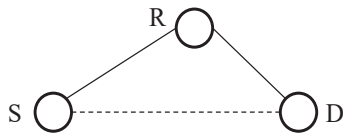

Figure 4.11: A three-terminal scenario

cation in a three-terminal scenario when applying BPSK modulation are derived. By comparing the BER expressions, better performance with cooperative communication is achieved. The authors in [4] consider Simultaneous Wireless Information Power Transfer (SWIPT) in cooperative communication. [5] proposes a Device-to-Device (D2D) cooperative communication management system for use in a disaster area with the help of an energy harvesting relay. Nevertheless, both methods save energy in cooperative communication by sacrificing BER performance.

The three-terminal scenario is shown in Figure 4.11. In a flat Rayleigh fading wireless environment, the channel coefficients from S to R, and R to D are h_{SR} and h_{RD}, respectively. The transmit power at S and R are P_{S} and P_{R}. The power of Additive White Gaussian Noise (AWGN) is N_0. Thus, the average received Signal-to-Noise Ratio (SNR) at R is $\mathrm{snr}_{\mathrm{SR}} = \mathrm{E}[|h_{\mathrm{SR}}|^2 P_{\mathrm{S}}/N_0]$. Similarly, $\mathrm{snr}_{\mathrm{RD}} = \mathrm{E}[|h_{\mathrm{RD}}|^2 P_{\mathrm{R}}/N_0]$. And $\mathrm{E}[|h_{\mathrm{SR}}|^2] = 1/L_{\mathrm{SR}}^{\alpha}$ and $\mathrm{E}[|h_{\mathrm{RD}}|^2] = 1/L_{\mathrm{RD}}^{\alpha}$, where L_{SR}, L_{RD} are the distances from S to R, and R to D respectively, and α is the path loss exponent. Hence, $\mathrm{snr}_{\mathrm{SR}} = P_{\mathrm{S}}/(L_{\mathrm{SR}}^{\alpha} N_0)$ and $\mathrm{snr}_{\mathrm{RD}} = P_{\mathrm{R}}/(L_{\mathrm{RD}}^{\alpha} N_0)$.

In a DF relay, the BER should be calculated in two parts. If node R incorrectly decodes a signal from node S, the probability is $\mathrm{p}(\mathrm{snr}_{\mathrm{SR}})$. Consequently, node D has to decode from the noise, thus the error probability is $\frac{1}{2}$. If node R decodes the signal correctly, the probability is $1 - \mathrm{p}(\mathrm{snr}_{\mathrm{SR}})$. The error probability of decoding at node D is $\mathrm{p}(\mathrm{snr}_{\mathrm{RD}})$. Hence, the overall BER is

$$\begin{aligned} \mathrm{BER_{DF}} &= \frac{1}{2}\mathrm{p}(\mathrm{snr_{SR}}) + [1 - \mathrm{p}(\mathrm{snr_{SR}})] \times \mathrm{p}(\mathrm{snr_{RD}}) \\ &= \frac{1}{2} - \frac{1}{4}(1 + \sqrt{\frac{\mathrm{snr_{SR}}}{1 + \mathrm{snr_{SR}}}}) \times \sqrt{\frac{\mathrm{snr_{RD}}}{1 + \mathrm{snr_{RD}}}} \end{aligned} \tag{4.12}$$

In cooperative communication, we take advantage of the weak signal from the direct link between nodes S and D to improve the performance. The average received SNR at D from S is $\mathrm{snr_{SD}} = P_{\mathrm{S}}/(L_{\mathrm{SD}}^{\alpha} N_0)$, where L_{SD} is the distance between S and D. The BER calculation is similar to the DF relaying scheme. When R decodes a signal from S incorrectly, the error probability at D is $\frac{1}{2}\mathrm{p}(\mathrm{snr_{SR}})$. When R decodes correctly, assume Maximal Rate Combination (MRC) is performed at D, and the error probability of decoding at D is $\mathrm{p}(\mathrm{snr_{RD}} + \mathrm{snr_{SD}})$. Therefore, the overall BER is

$$\begin{aligned} \mathrm{BER_{CC}} &= \frac{1}{2}\mathrm{p}(\mathrm{snr_{SR}}) + [1 - \mathrm{p}(\mathrm{snr_{SR}})] \times \mathrm{p}(\mathrm{snr_{RD}} + \mathrm{snr_{SD}}) \\ &= \frac{1}{2} - \frac{1}{4}(1 + \sqrt{\frac{\mathrm{snr_{SR}}}{1 + \mathrm{snr_{SR}}}}) \times \sqrt{\frac{\mathrm{snr_{RD}} + \mathrm{snr_{SD}}}{1 + \mathrm{snr_{RD}} + \mathrm{snr_{SD}}}} \end{aligned} \tag{4.13}$$

For the same values of $\mathrm{snr_{SR}}$ and $\mathrm{snr_{RD}}$, $\mathrm{BER_{DF}} > \mathrm{BER_{CC}}$, which means cooperative communication outperforms DF relaying in terms of BER. Furthermore, to meet the same BER requirement, cooperative communication consumes less energy than DF relaying.

We now investigate the energy efficiency performance of DS cooperative communication. The distances are L_{SR} =20m, L_{RD} =20m and L_{SD} =28.28m. The path loss exponent α =4. The outage threshold for SNR at D is snr_{th} =0dB. In the DF relay and DS cooperative communication, $\mathrm{snr_{SD}} < \mathrm{snr}_{th}$ and $\mathrm{snr_{SD}}$ =-1dB.

Figure 4.12 depicts the comparative energy consumption results. Observe the one-way wireless transmission under DF relaying and the DS cooperative communication method, changing $\mathrm{snr_{RD}}$ from 0 to 6dB. With the same BER performance requirement,

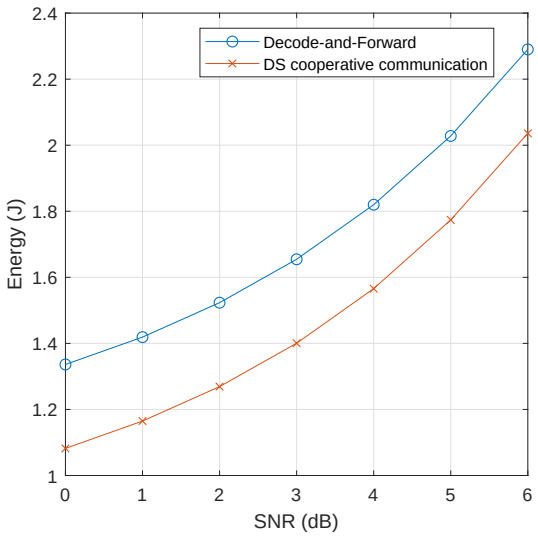

Figure 4.12: Energy consumption comparison

both methods transmit the same 20Mb of data. The transmission rate is the same, being 1Mb/s. By increasing $\mathrm{snr}_{\mathrm{RD}}$ from 0 to 6dB, the overall energy consumption of both DF and DS increase. However, DS consumes less energy than DF due to the help of cooperative communication.

4.4 Cooperative Communication Related Mathematical Analysis

Although cooperative communication can improve the performance in a wireless network, it raises some questions. One question concerns how cooperative communication structures are identified and established. As we know, to investigate the performance of a wireless network, one effective way is to analyse the network topology. Knowledge of the network topology is important as it determines the node connectivity status, the node's neighbours, the node degree, and overall distribution and location of nodes in a wireless network. It provides important and effective information to support further tasks, such as power control, interference cancellation, routing design and cross layer

protocol design. In [6] several practically relevant factors are considered in modelling topology links, including the remaining battery levels of the nodes, traffic dependent link blocking, log-normal shadowing during transmission, directional antennas, and terrain variations due to obstacles.

To find how many cooperative communication patterns are constructed in a given scenario, consider this problem from the perspective of the network topology. In [7], numerical analysis of r-neighbour graphs are provided. Inspired by it, this section presents a mathematical analysis to determine the average number of established cooperative communication structures, which is relevant to the performance gain.

In this section, mathematical expressions for theoretically determining the number of cooperative communication structures constructed within a wireless network are derived. We only consider three-terminal cooperative communication entities.

Suppose a wireless network with n nodes is uniformly distributed over a rectangular region with area A. The average node density is $\mu = \frac{n}{A}$. The maximum transmission radius of each node is R. Assume that transmission range is the same for every node.

First, we derive the average number of cooperative communication clusters per node. As the node distribution is assumed to be uniform, it is easy to determine the number of nodes present at a certain distance from a given node. Observe an arbitrary node s within the deployment area. As shown in Figure 4.13, the average number of nodes at distance x from node s is

$$N(x) = 2\pi\mu x \mathrm{d}x \tag{4.14}$$

The average number of cooperative communication clusters constructed between nodes from distance x and node s is

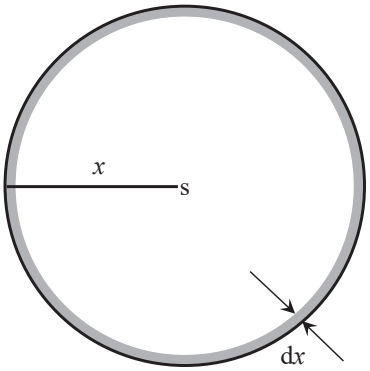

Figure 4.13: A circular strip at distance x from node s

$$N_A(x) = N(x) \times \mathrm{P}_A(x) \tag{4.15}$$

where $\mathrm{P}_A(x)$ is the probability of that a cooperative communication cluster is constructed between one node t at a distance x from node s. Cooperative communication can only be established with nodes outside the transmission range of s, $x > R$. If a node t is within the farthest distance $2R$ of two relay hops from node s, when there exists another relay in the common transmission area, cooperative communication is established. Figure 4.14 illustrates the establishment of a cooperative communication cluster. The expected number of cooperative communication clusters for a node s is

$$C = \int_R^{2R} N(x) \times \mathrm{P}_A(x)\mathrm{d}x \tag{4.16}$$

And the average number of cooperative communication clusters for the network is

$$N_A = \frac{n \times C}{2} \tag{4.17}$$

The last step is to derive an expression for $\mathrm{P}_A(x)$. The area of the common transmission ranges in Figure 4.14 is

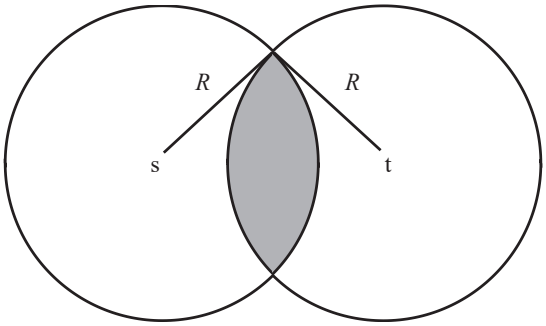

Figure 4.14: Illustration of establishing a cooperative communication cluster

$$A_c = R^2[\pi - 2\delta - \sin(2\delta)] \tag{4.18}$$

where $\delta = \sin^{-1}(\frac{x}{2R})$. Since the nodes are uniformly distributed, the probability of a certain number of nodes existing in an area obeys the Poisson distribution. Therefore, the probability that there exists at least one node in the common area A_c is

$$\mathrm{P}_A(x) = 1 - \mathrm{e}^{-\mu A_c} \tag{4.19}$$

Let $A_c = R^2\gamma$, where $\gamma = \pi - 2\delta - \sin(2\delta)$, hence

$$\begin{aligned} C &= \int_R^{2R} 2\pi\mu x(1 - \mathrm{e}^{-\mu R^2\gamma})\mathrm{d}x \\ &= 3\pi\mu R^2 - \int_R^{2R} 2\pi\mu x\mathrm{e}^{-\mu R^2\gamma}\mathrm{d}x \end{aligned} \tag{4.20}$$

4.5 Dual Sampling Conclusions

A Dual Sampling method is proposed in this chapter. Firstly, reducing the transmission phases in two-way three-terminal communications with the DS method is explained.

The information contained within the even sampling instants is the main factor that affects the performance of the DS scheme. Simulation results show that the DS method performs effectively at the relay node. Secondly, the BER expressions for both DF relaying and DS cooperative communication in a one-way transmission three-terminal scenario are derived. The derivations reveal the potential energy efficiency of DS cooperative communication over DF. Finally, an expression for estimating the number of cooperative clusters in a wireless network is presented. Additional simulations reveal the energy saving and delay reduction benefits of the proposed DS cooperative communication method.

References

[1] Pilz J, Mehlhose M, Wirth T, et al, "A Tactile Internet demonstration: 1ms ultra low delay for wireless communications towards 5G," 2016 IEEE Conference on Computer Communications Workshops (INFOCOM WKSHPS). IEEE, 2016: 862-863.

[2] Kim D Y, Kim S, Hassan H, et al. "Adaptive Data Rate Control in Low Power Wide Area Networks for Long Range IoT Services," Journal of Computational Science, 2017.

[3] X. Liu and W. Du, "BER-Based Comparison between AF and DF in Three-Terminal Relay Cooperative Communication with BPSK Modulation," 2016 12th International Conference on Mobile Ad-Hoc and Sensor Networks (MSN), Hefei, 2016, pp. 296-300.

[4] Z. Chu, M. Johnston, and S. L. Goff, "SWIPT for wireless cooperative networks," Electron. Lett., vol. 51, no. 6, pp. 536538, 2015.

[5] Z. Chu et al., "D2D cooperative communications for disaster management," 2017 24th International Conference on Telecommunications (ICT), Limassol, 2017, pp. 1-5.

[6] A. Farago, "Topology analysis of multi-hop wireless networks," 2015 IEEE 16th

International Conference on High Performance Switching and Routing (HPSR), Budapest, 2015, pp. 1-6.

[7] A. Rahman, N. R. Rasha, I. Ahmed, et al, "Modeling sparsity of planar topologies for wireless multi-hop networks," 2015 13th International Symposium on Modeling and Optimization in Mobile, Ad Hoc, and Wireless Networks (WiOpt), Mumbai, 2015, pp. 339-346.

Chapter 5

Cache Migration Protocol

The decoding of information from the overlapping signals is based on the network coding mechanism, which needs information to be stored at the transmission destinations. This requirement fits well with the features of ICN, where content is stored throughout the network. Generally for an ICN, various content is distributed. Furthermore, it is common to have different content transmissions happening through the same relay node simultaneously. With the help of the DS method, the impact of signal asynchrony can be alleviated. To equip ICN nodes with a DS capability for simultaneous transmissions is relatively easy to achieve. In this chapter, the preparation procedure needed to exploit DS-based simultaneous transmissions in ICN is explained.

For ICN with multiple caches systems, a global caching gain can be obtained by coded caching during the cache placement stage between the content originator and cache routers. Additionally, the use of a distributed, simultaneous transmission technique, and dynamic context supported protocol can provide extra performance gains. In this chapter, a Cache Migration Protocol (CMP) to support the dynamic simultaneous transmission during the content delivery stage between cache routers and consumers in a distributed manner is proposed. The design of CMP is evaluated via simulations using OPNET. The simulations show that CMP is able to select appropriate nodes for

supporting the DS method when the network context is changed.

For this chapter, the contributions can be summarized as follows:

- CMP is proposed to distributively form a suitable network structure considering the dynamic network context for support of the DS method.
- The design of CMP supports the re-establishment of an appropriate network structure in a dynamic environment when consumers are moving, which improves the resistance of CMP to link breaks due to mobility.
- The robustness of CMP functions are evaluated under various scenarios within the OPNET [1] platform.

5.1 System Model

A coded caching network is composed of one content originator, multiple cache routers and consumers. The cache routers are used for caching content to meet the requests of consumers locally instead of the remote originator. Regardless of their positions, all cache routers share a common bottleneck link with the originator, as illustrated in Figure 5.1. The cache routers request content from the originator based on the consumers' Interest packets. The originator then codes the multiple transmissions towards the cache routers in order to achieve a global transmission gain. However, due to the energy and hardware constraints, the content delivery stage between cache routers and consumers is typically realized by a multi-hop relay network. In this chapter, we focus on the content delivery stage rather than the content placement stage.

A specific example is shown in Figure 5.2 depicting the transmission methods employed during the content delivery stage. Assume all the devices work in half-duplex mode. In addition, assume cache routers and consumers are able to forward content as well. Cache routers 1 and 3 already contain cached content as a result of the content place-

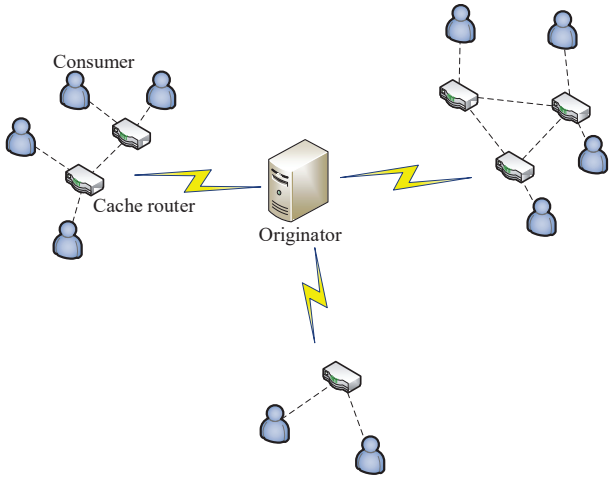

Figure 5.1: A coded caching network model

ment stage. Some new requests for content by the consumers may then occur, that is consumer 1 requests the content in cache router 3, and consumer 2 wants the content in cache router 1. The number within each arrow indicates the corresponding transmission phase. For the traditional request-respond NDN [2] content delivery method, it experiences four transmission phases. However, if the content 'migrates' from cache router 3 to cache router 2, then we can leverage a simultaneous transmission technique, like the DS method [3] at consumer 3, permitting simultaneous transmissions from both cache routers 1 and 2 and then forwarding the mixed signal to consumers 1 and 2 in the next transmission phase. Thus only two transmission phases are required, leading to a 50% reduction which reveals the extra performance gain obtained by the mechanism. Actually, cache router 2 requests the content from the originator, and it looks like a cache 'migration' from cache router 3[1]. It is reasonable to design a protocol which can realise the network context change and form the appropriate network structure to enable the DS method. This is the basic principle behind CMP.

In the scenario shown in Figure 5.2, transmission of different content occurs at the relay node consumer 3. With knowledge of the DS method, simultaneous transmis-

[1]It should be noted that the transmission mechanism between the originator and cache routers can be realized in various ways depending on the scenario. For example, a wired infrastructure could be in place which results in little cost when migrating content between originators and the cache router nodes. However, the transmission between the originator and cache routers is beyond the scope for this work.

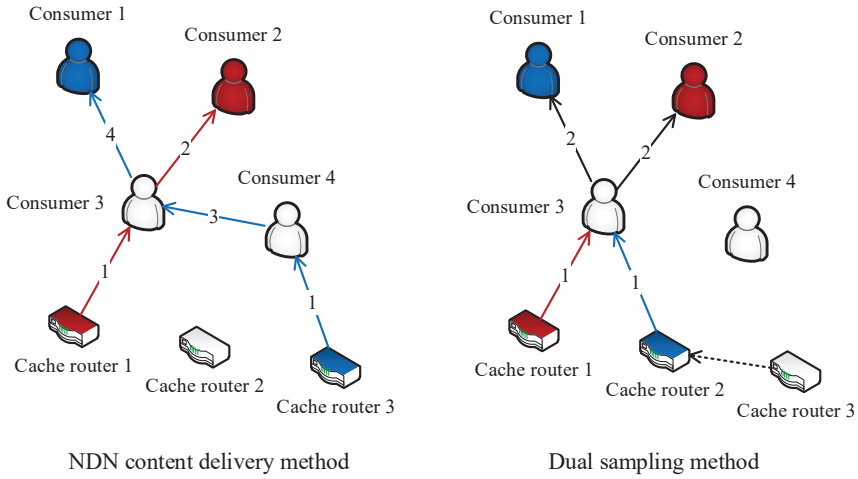

Figure 5.2: Case 7N2C - transmission methods comparison

sions can be supported thus reducing the number of transmission phases as well as the latency. The operation of CMP is explained in the next section.

5.2 Cache Migration Protocol

Since the DS method is able to reduce transmission phases, it is reasonable to design a protocol that allows the network to self-organise to form an appropriate structure for cache migration. The proposed CMP scheme is based on the NDN forwarding paradigm. In the scenarios discussed in this chapter, assume that only cache routers have a Content Store (CS) and consumers operate without a CS.

CMP is suitable for various consumers that request different content simultaneously. Interest packets are generated for each different piece of content that is required. For an intermediate consumer, when it receives Interest packets relating to two different pieces of content the first time, it will refer to the Forwarding Information Base (FIB) and decide whether to send out a CACHE SELECTION message or not. The FIB is formed by periodically exchanging the Hello messages. If there exists two entries in FIB pointing to cache routers that can potentially be sources for the two pieces of con-

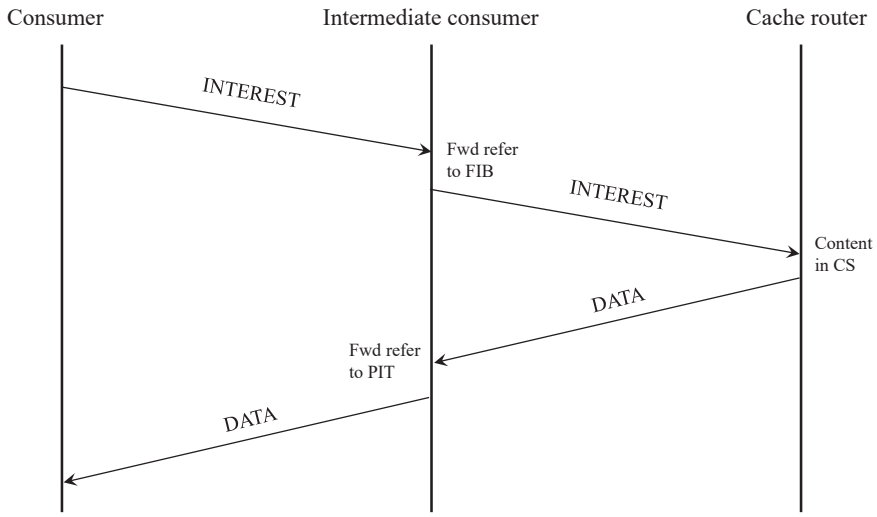

Figure 5.3: NDN content retrieval and delivery procedure

tent, then the CACHE SELECTION message is sent out containing the content migration configuration information. However, if less than two cache routers are found in the FIB, no CACHE SELECTION message will be generated, and the intermediate consumer will follow the NDN process. Upon receiving the CACHE SELECTION message, a cache router looks for its corresponding information to obtain the content name for cache migration, then it will start the cache migration process and prepare itself for the DS transmission. CMP always tries to find appropriate cache routers for cache migration in order to support the DS transmission before the NDN forwarding process is invoked. This increases the probability of utilizing the wireless transmission resources more efficiently. Compared to NDN, CMP only introduces the CACHE SELECTION message which only slightly increases the control overhead burden.

The fundamental content retrieval and delivery procedure for NDN is shown in Figure 5.3. Only when different Interest packets arrive at the intermediate consumer, will the procedure shown in Figure 5.4 for CMP be triggered.

The selections made by the intermediate consumers are executed in a distributed manner. The procedure starts from the consumers who request content, and is com-

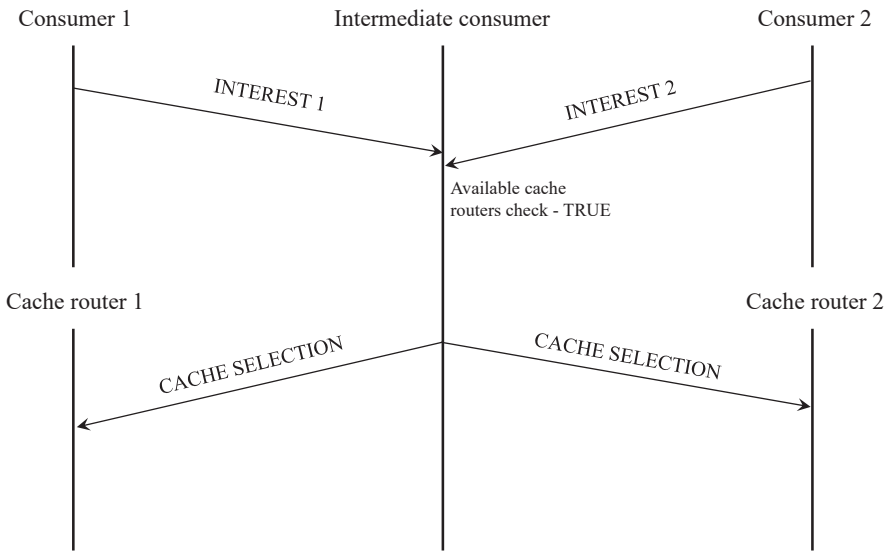

Figure 5.4: Message exchange in CMP

pleted by selecting the appropriate cache routers for migration. This process seamlessly supports the DS method. Furthermore, take the example shown in Figure 5.2 as a clearer illustration of the CMP process.

Consumers 1 and 2 generate Interest packets asking for different content. Consumer 3 will receive the two Interest packets and then looks up its FIB. There exists two entries for cache routers 1 and 2 that are suitable for the cache migration. Thus consumer 3 sends out a CACHE SELECTION message. On receiving the CACHE SELECTION message, since cache router 1 already caches one content, cache router 2 will be chosen for the cache migration. Therefore, cache routers 1 and 2, together with consumer 3 are able to effectively support the DS simultaneous transmission technique.

5.3 Two Further Examples

As illustrated in Figure 5.5, consumers 1 and 2 request content cached in cache routers 3 and 1, respectively. During the content delivery stage, if the DS method is used at

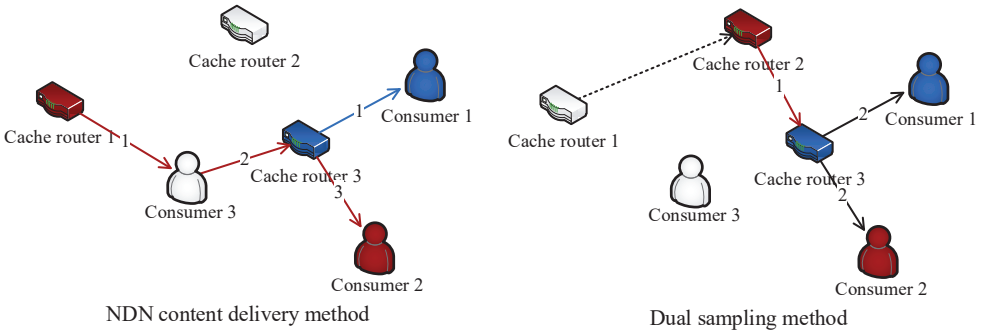

Figure 5.5: Case 6N2C

cache router 3, the appropriate cache migration is from cache router 1 to cache router 2. By comparing the transmission phases, it is reduced from 3 to 2. This situation is supported by CMP. Upon receiving the two Interest packets from consumers 1 and 2, the cache router 3 looks up its FIB and chooses cache router 2 for cache migration by sending the CACHE SELECTION message. This case shows that the cache router can also exploit CMP, which extends its applicability.

The scenario shown in Figure 5.6 is an extension of the scenario in Figure 5.2. Besides consumers 1 and 2, consumers 7 and 8 also request content. By leveraging DS at consumers 3 and 6, the number of transmission phases for content delivery can be reduced from 4 to 2. This case shows that CMP is able to form multiple structures concurrently which simplifies complex transmission scenarios.

CMP facilitates cache migration by exploiting simultaneous transmissions when a suitable network structure can be formed. This then reduces the number of transmission phases. CMP is suitable for multiple caches system where different consumers are requesting content cached across different cache routers.

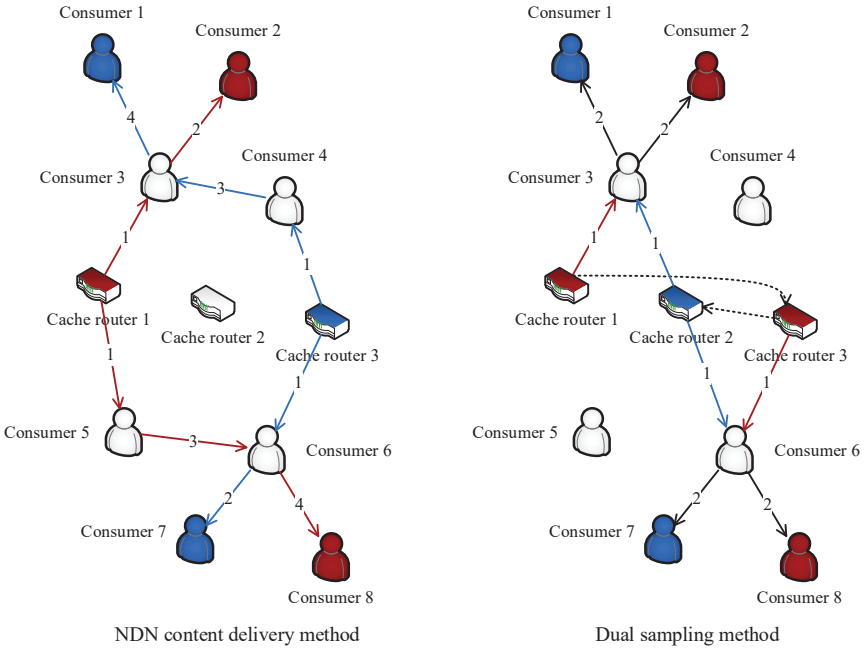

Figure 5.6: Case 11N4C - CMP supports four consumers

5.4 CMP Supports Consumer Mobility

In the previous illustrations, all the nodes are stationary and the CMP scheme manages to provide appropriate cache migration. The work mentioned in [4] also considers mobility management of nodes. Thus, in the proposed CMP approach, node mobility is also considered. We focus on the case when the originator and cache routers are stationary but the consumers may move. In the CMP scheme, even when the consumer moves and breaks the connections, CMP is able to detect the link break before re-selecting the cache routers for another cache migration.

In this section, it demonstrates that when the consumer which requests the content moves, CMP can effectively re-establish the network structure for cache migration. For a more complex case, such as when the intermediate consumer moves, the consumers will find another node as a replacement. If no suitable nodes are found, the consumers have to wait until another node moves to enable the network structure to be re-formed. For now, we present a basic example when the consumer requesting content is moving.

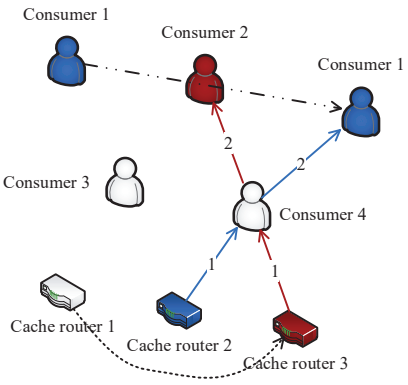

Figure 5.7: Case 7N2C_MOBILE - CMP with mobile consumer

As shown in Figure 5.7, during the content delivery phase, consumer 1 moves to a new position. The link between consumers 1 and 3 is disconnected. Then consumer 3 sends a CONSUMER LEAVE NOTIFICATION message to the uplink cache routers 1 and 2 to stop content transmissions. Meanwhile, consumer 4 receives the Interest packets from consumers 1 and 2, and then send the CACHE SELECTION message to cache router 3 for the migration regarding the new position of consumer 1.

5.5 Cache Migration Protocol Performance Evaluation

In this section, we provide a performance comparison of CMP incorporating DS and the conventional NDN method. Both methods are implemented on the network simulation platform OPNET [1]. This tool is suitable for implementing node functionality and simulating network behaviour, as well as collecting statistics. NDN transmissions are implemented via the content request and content delivery procedure. With the CMP-DS approach, all the new message types and corresponding message handling mechanisms are implemented as described in this chapter. Besides the average end-to-end delay, another metric is compared, the number of transmissions, which is defined as the number of data transmissions per unit time for the given network.

Regarding the performance comparison, some basic cases are considered first. In

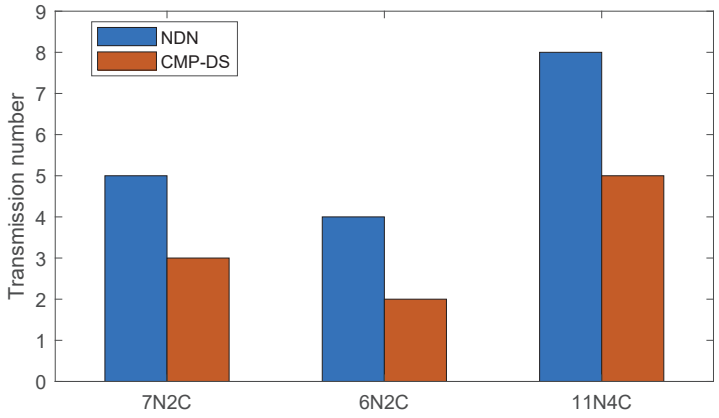

Figure 5.8: Transmission number comparison

order to make it clear and simple, we name the cases based on the network structure. Therefore, the case shown in Figure 5.2 is named 7N2C (Seven Nodes Two Consumers), for the Figure 5.5 case it is 6N2C, and in the Figure 5.6 case it is 11N4C.

Figure 5.8 shows a comparison of the number of transmissions between NDN and CMP-DS for the above three cases during the stable transmission period. For the NDN content delivery method, the transmission number includes the cache routers and intermediate node transmissions. With the CMP-DS method, the transmission number consists of cache routers and intermediate consumer transmissions. By observing the simulation results, the transmission number with CMP-DS is less than that of NDN. Using the DS method permits merging of different incoming signals in one transmission phase, rather than forwarding them sequentially as with NDN. A lower transmission number means less energy and network resources are consumed.

Assume the data rate of a cache router is 2 Mbit/s, the absolute data rate is of little importance, and the simulation duration is 5 minutes for both NDN and CMP-DS methods. The real time delay and average delay comparison results are shown in Figure 5.9, 5.10, and Figure 5.11, respectively. For each case, the system evolves to a steady state as the time-window average delay curve plateaus. In each case, the CMP-DS method outperforms NDN significantly. This is because the NDN method only allows sequential

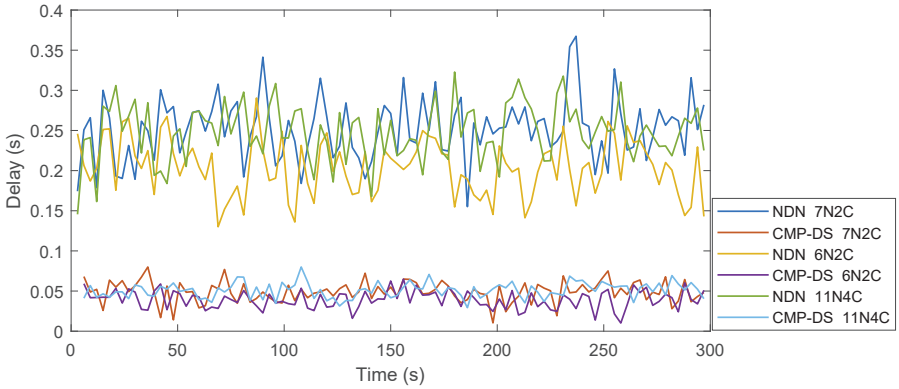

Figure 5.9: Delay comparison

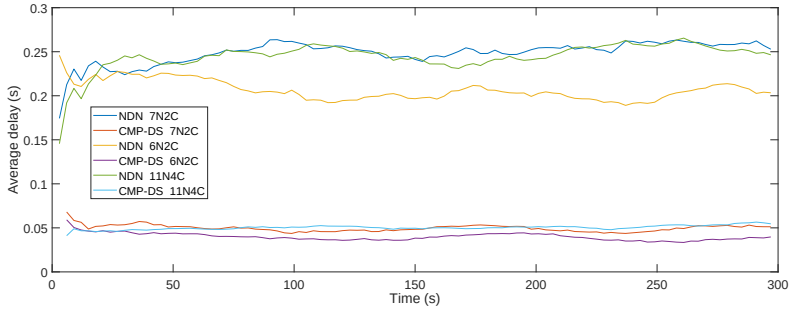

Figure 5.10: 1 min time-window average delay comparison

data transmission and thus needs a medium access control mechanism to avoid the collisions. Conversely, CMP-DS supports simultaneous transmissions. Thus the CMP-DS method can effectively reduce the delay during the content delivery phase.

Next simulations are carried out with a more complex scenario, as shown in Figure 5.12, named 50N8C (Fifty Nodes, Eight Consumers). There are eight consumers distributed throughout the network, node_1, node_3, node_12, node_19, node_25, node_30, node_44 and node_46. For the NDN method, node_16 and node_38 are cache routers with cached content. The data rate at a cache router is 2M bits/s, and each simulation lasts for 2 minutes. The scenario with more nodes can be an IoT ICN system [6] or a mobile ad hoc ICN network [7]. The total number of nodes and the overall topology

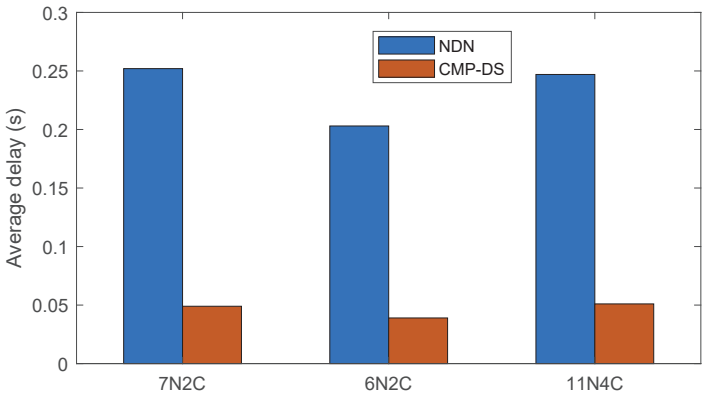

Figure 5.11: Average delay comparison

of the system are not the most relative factors that affect the execution of CMP. It is the local neighbour distribution at a consumer that determines whether CMP can be properly triggered or not. If, for the intermediate consumer, there are available idle neighbour cache routers for cache selection, then CMP will operate. If no such cache router exists, the intermediate consumer will forward the Interest packet searching for the content, in the same manner as NDN does.

As shown in Figure 5.13, CMP-DS performs better than NDN in the real time delay. And in Figure 5.14, the steady state of the system is achieved as the time-window average delay curve plateaus. The system operates CMP quickly, such that within 2 minutes it converges to a relatively steady state. Furthermore, as shown in Figure 5.15, CMP-DS outperforms NDN significantly, both in terms of average delay and average throughput. In NDN, each consumer has to retrieve the content from the cache routers which are multi-hops away. In contrast, CMP-DS permits the consumer to select nearby cache routers for cache migration. Additionally, the transmission phases can be reduced with the CMP-DS method. Hence, the delay with CMP-DS is less than that in NDN, and this results in higher average throughput for CMP-DS than NDN. With more consumers in a complex network, the delay and throughput gains brought about by CMP-DS further increase.

It is worth pointing out that enabling DS in NDN without cache migration can

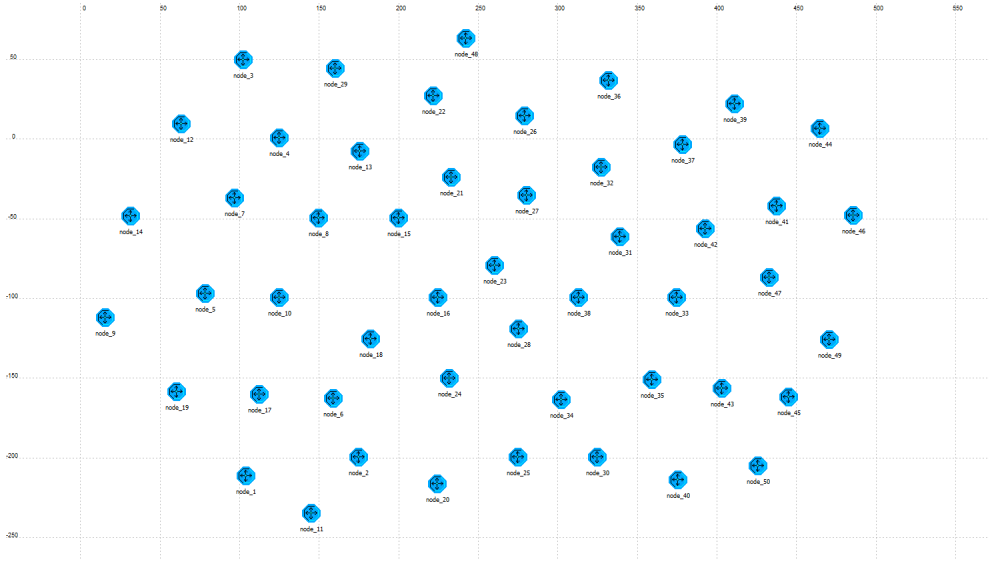

Figure 5.12: Case 50N8C topology

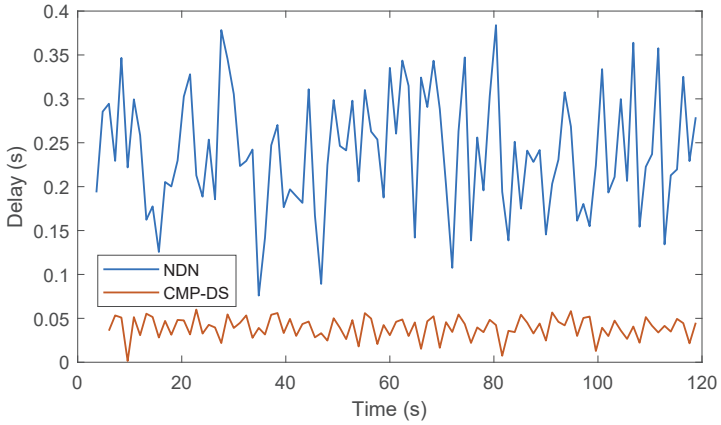

Figure 5.13: Delay comparison for case 50N8C

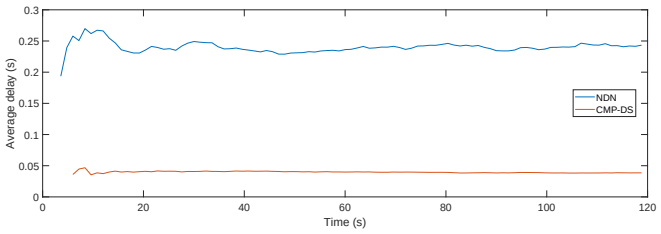

Figure 5.14: 1 min time-window average delay comparison for case 50N8C

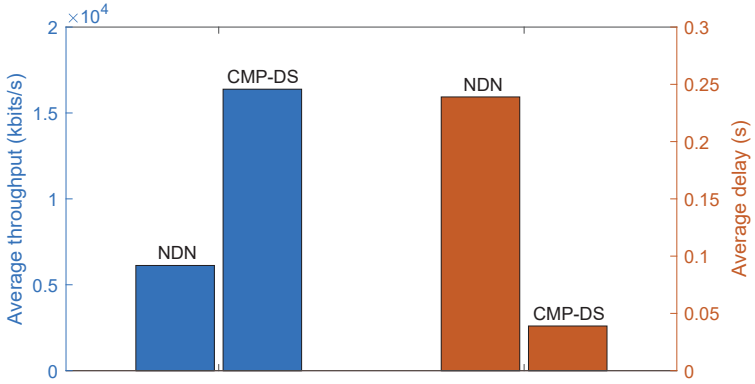

Figure 5.15: Performance comparison for case 50N8C

reduce the content delivery latency as well. However, this costs more in terms of the number of operations to deal with the signals' asynchrony and becomes less efficient compared with CMP-DS. The signals' asynchrony affects the performance of DS and handling the asynchrony requires additional processing [3]. For DS in NDN, simultaneous transmission can happen between a cache router and an intermediate consumer. The consumer needs to receive and decode the data packets before commencing the simultaneous transmission, hence it is more likely to cause signal asynchrony. For CMP-DS, simultaneous transmission occurs between the cache routers. Being the source of the data packets, it is more feasible to achieve signal synchronization with the cache routers. Therefore, the cache migration approach is more suitable for leveraging the DS method.

To evaluate the CMP-DS performance in a mobile scenario, consider the case in Figure 5.7 as 7N2C_MOBILE. Consumer 1 starts moving at 30 seconds, with a speed of 6.1m/s lasting for 36s. The simulation lasts for 5 minutes, and the results are shown in Figure 5.16. The delay has breakpoints and the transmission number drops due to the disconnection caused by the movement of consumer 1. After re-selecting the cache routers for cache migration, the content delivery process then recovers. CMP is able to re-establish the content delivery structure when the consumer moves.

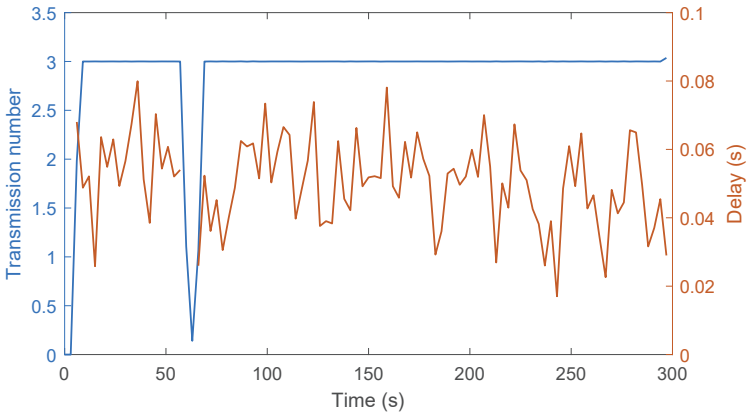

Figure 5.16: CMP-DS performance for case 7N2C_MOBILE

5.6 Cache Migration Protocol Conclusions

Coded caching is a promising paradigm which exploits coding multiple transmissions, providing a global transmission gain. In this chapter, a Cache Migration Protocol for coded caching networks to support the Dual Sampling method during the content delivery stage between the cache routers and consumers is proposed. We first demonstrate the design of the proposed protocol, including the packet flow handling and the scheme's implementation in OPNET. We then compare CMP-DS against traditional NDN content delivery in terms of number of transmissions, average end-to-end delay and average throughput. As CMP manages to select appropriate nodes for cache migration, the DS method is supported seamlessly. With fewer transmission phases, CMP-DS outperforms the traditional NDN method. It also shows that CMP is able to re-select nodes for cache migration when a consumer moves. CMP provides an effective approach for exploiting simultaneous transmissions to achieve extra performance gains, especially in terms of reduced transmission latency.

5.7 Cache Migration Protocol in Random Waypoint Mobility Model

This section focuses on the relay selection problem for CMP, especially in a random mobility environment. The relay is the node connecting the cache routers and the consumers requesting the content, such as consumer 3 shown in Figure 5.2. Assume the nodes that can be selected as a relay are mobile, though the cache routers and consumers are stationary. The most commonly used random mobility model in the wireless environment is the Random Waypoint (RWP) model. In this stochastic model, each mobile node of the system chooses uniformly at random a destination point in a rectangular deployment region Q. A node moves to this destination with a velocity v chosen uniformly at random in the interval $[v_{\min}, v_{\max}]$. When it reaches the destination, it remains static for a predefined time t_p and then starts moving again according to the same rule. In this section, RWP is used to model the random mobility of nodes. The following parameters describe a simulation set-up with generalized RWP mobility in a complete manner:

- size and shape of the deployment region Q,
- initial spatial node distribution $f_{init}(\mathrm{x})$,
- the probability p_s that a node remains static during the whole process, with $0 \leq p_s \leq 1$,
- probability density function $f_{T_p}(t_p)$ of the pause time, and
- minimum speed and maximum speed: $0 \leq v_{\min} \leq v_{\max}$.

The initial node distribution, $f_{init}(\mathrm{x})$ is used to place nodes at the beginning of a simulation in Q. In general, it is different from a uniform distribution. Next, based on the description of the RWP model, the probability that a typical CMP structure remains connected is analysed. This connectivity means that the relay node manages to receive

the data from the cache routers, and sends it to the consumers.

The node distribution of the generalized RWP model in a square region $Q = [0,1]^2$ is derived in [5] as:

$$f_{XY}(x,y) = f_s(x,y) + f_p(x,y) + f_m(x,y) \tag{5.1}$$

where $f_s(x,y) = p_s \times f_{init}(x,y)$ is the distribution of a node that is static during the entire network operational time. $f_p(x,y) = (1-p_s)p_p$ is the probability of a node in the pause status. For $v_{\min} = v_{\max} = v > 0$, $p_p = \frac{E[T_p]}{E[T_p]+E[L]/v}$. $f_m(x,y) = (1-p_s)(1-p_p)f_m^0(x,y)$ is the distribution of a node in the mobility status. And $f_m^0(x,y)$ is the following normalized probability density function:

$$f_m^0(x,y) = \begin{cases} f_m^*(x,y) & 0 < x \le \frac{1}{2},\ 0 < y \le x \\ f_m^*(y,x) & 0 < x \le \frac{1}{2},\ x \le y \le \frac{1}{2} \\ f_m^*(1-y,x) & 0 < x \le \frac{1}{2},\ \frac{1}{2} \le y \le 1-x \\ f_m^*(x,1-y) & 0 < x \le \frac{1}{2},\ 1-x < y \le 1 \\ f_m^*(1-x,y) & \frac{1}{2} \le x < 1,\ 0 < y \le 1-x \\ f_m^*(y,1-x) & \frac{1}{2} \le x < 1,\ 1-x \le y \le \frac{1}{2} \\ f_m^*(1-y,1-x) & \frac{1}{2} \le x < 1,\ \frac{1}{2} \le y \le x \\ f_m^*(1-x,1-y) & \frac{1}{2} \le x < 1,\ x \le y < 1 \\ 0 & \text{otherwise} \end{cases} \tag{5.2}$$

where $f_m^*(x,y)$ is defined on $Q^* = \{(x,y) \in [0,1]^2 | (0 < x \le \frac{1}{2}) \wedge (0 < y \le x)\}$, with

$$
\begin{aligned}
f_m^*(x,y) = 6y + \frac{3}{4}(1-2x+2x^2)(\frac{y}{y-1} + \frac{y^2}{(x-1)x}) \\
+ \frac{3y}{2}[(2x-1)(y+1)\ln(\frac{1-x}{x}) \\
+ (1-2x+2x^2+y)\ln(\frac{1-y}{y})]
\end{aligned}
\tag{5.3}
$$

To theoretically analyse the connectivity status for CMP in an RWP environment, it is equivalent to calculating the probability that at least one node located within the common transmission area among the cache routers and consumers that is eligible for relay selection.

Assume that the cache routers and consumers are located at the four vertices of a square with side of length 1. The transmission radius for all nodes are the same R. The common transmission area is the intersection region of the four circular transmission ranges, as illustrated in Figure 5.17. In order to ensure the existence of the common transmission area, while the cache router and consumer cannot communicate directly with each other, R should be $\frac{1}{\sqrt{2}} \leq R < 1$.

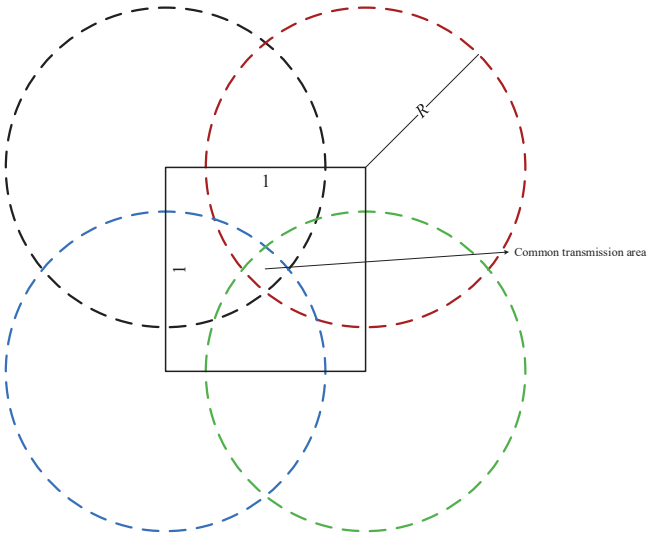

Figure 5.17: Common transmission area

After calculation, the common transmission area can be expressed as

$$A_c = 1 - 2\sqrt{R^2 - \frac{1}{4}} + (4\theta - \pi)R^2 \tag{5.4}$$

where $\theta = \arccos \frac{1}{2R}$. The relationship of R and A_c is shown in Figure 5.18. The common transmission area is directly related to the probability that a node lies in it, and the probability determines the degree that cache routers and consumers are connected via the relay node, which is an important metric when considering the transmission link status.

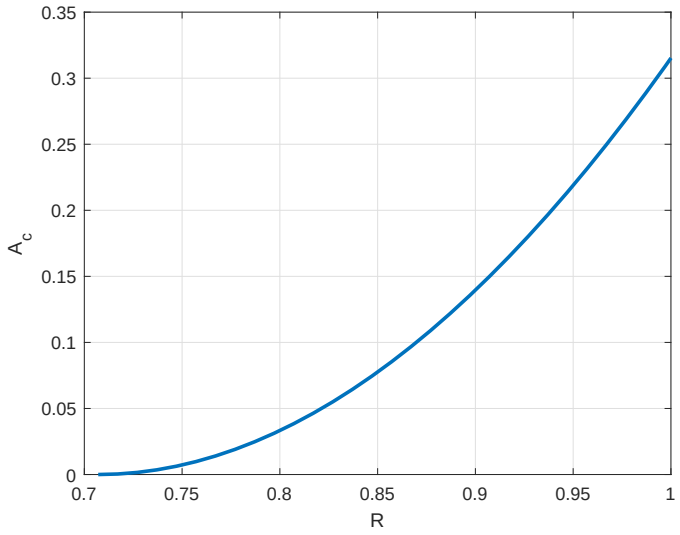

Figure 5.18: Relationship between R and A_c

In order to calculate the overall probability that a node is within the common transmission area, the probabilities of the three components, static, pause and mobility should be calculated separately. Assume the initial node distribution $f_{init}(x, y)$ is uniformly distributed, hence the static component of the probability is

$$P_s = p_s \times A_c \tag{5.5}$$

Since the waypoints are uniformly distributed, the pause component of the probability is

$$P_p = (1 - p_s) \times p_p \times A_c \tag{5.6}$$

and the mobility component is the following integration

$$P_m = (1 - p_s)(1 - p_p) \int_{x \in A_c} \int_{y \in A_c} f_m^0(x, y) \mathrm{dydx} \tag{5.7}$$

It is the integral of $f_m^0(x, y)$ over the common transmission area. And the common area can be approximated by the small square as shown in Figure 5.19. Due to the symmetry property, the integration over the small square is eight times that over the small triangle region Q_1. Therefore

$$P_m \approx 8(1 - p_s)(1 - p_p) \int_{x \in Q_1} \int_{y \in Q_1} f_m^*(x, y) \mathrm{dydx} \tag{5.8}$$

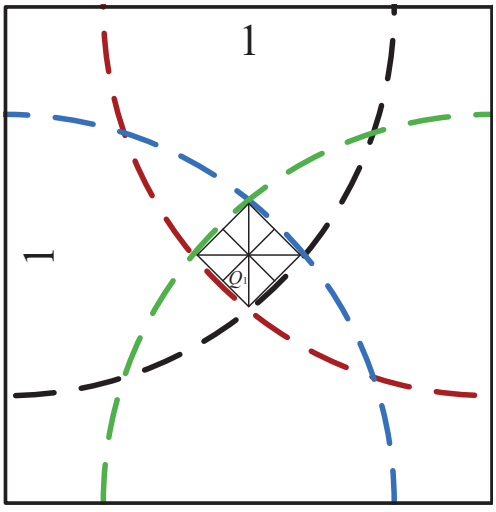

Figure 5.19: Approximation of common transmission area

For a clear demonstration, set $R = 0.9$ to theoretically analyse the connected probability of CMP. When $R = 0.9$, $A_c = 0.1396$ and $\int_{x \in Q_1} \int_{y \in Q_1} f_m^*(x, y) \mathrm{dydx} = 0.0326$. Thus the overall probability that a node locates within the common transmission area when

$R = 0.9$ is

$$\begin{aligned} P_{A_c} =& P_s + P_p + P_m \\ =& 0.1396p_s + 0.1396(1-p_s)p_p + 0.2608(1-p_s)(1-p_p) \end{aligned} \tag{5.9}$$

where $p_p = \frac{E[T_p]}{E[T_p]+E[L]/v}$ with $v_{\min} = v_{\max} = v > 0$, and $E[L] = 0.521405$. $E[L]$ is the expected distance between two nodes that are uniformly distributed in the region $[0,1]^2$.

The probability P_{A_c} with various pause time t_p, velocity v and static parameter p_s are shown in Figure 5.20, 5.21 and 5.22, respectively.

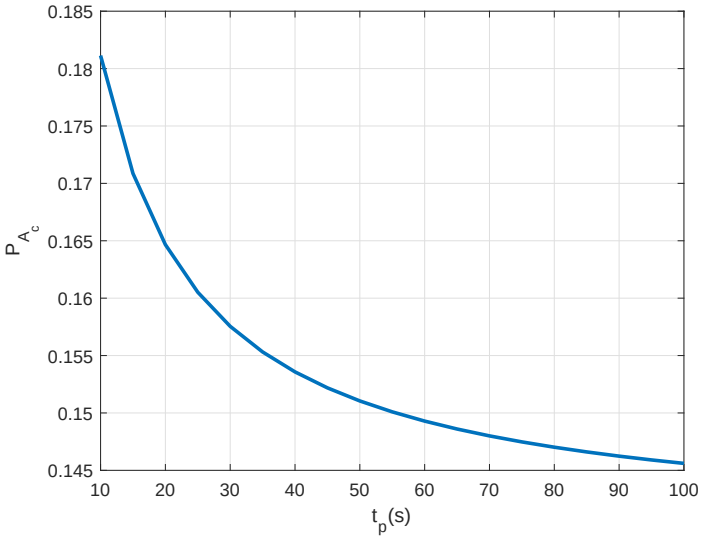

Figure 5.20: Various t_p, $p_s = 0$, $v = 0.1s^{-1}$

By observing the theoretical analysis results, with larger t_p and v, the probability P_{A_c} decreases. This is because the duration of the node movement decreases and the mobile node is more likely to be in the pause state. Increasing p_s will linearly decrease P_{A_c} as the node will more likely be static.

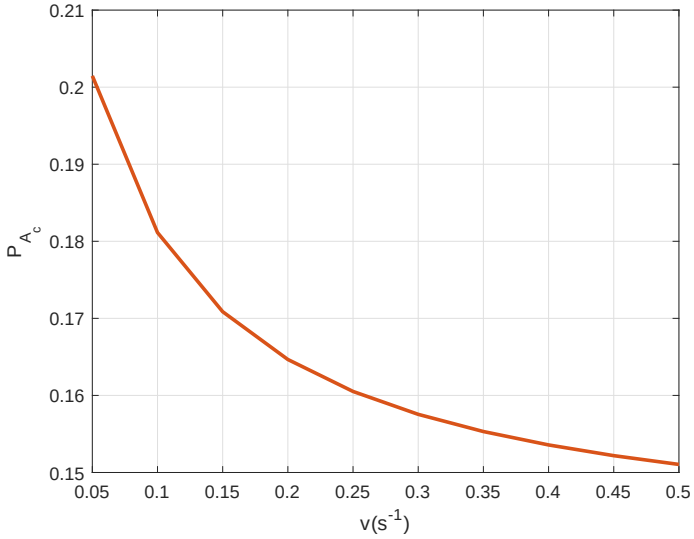

Figure 5.21: Various v, $p_s = 0$, $t_p = 10s$

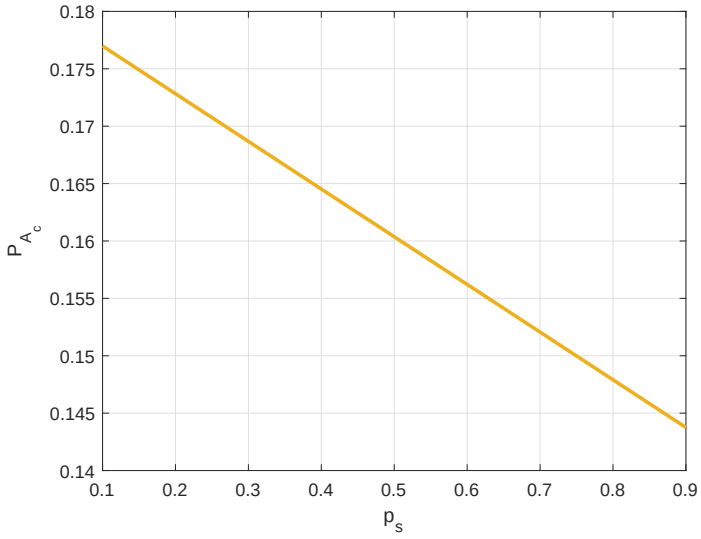

Figure 5.22: Various p_s, $v = 0.1s^{-1}$, $t_p = 10s$

When there are n nodes that can be selected as a relay located within the region $Q = [0, 1]^2$, and assume their movements to be independent of each other, then the connected probability of CMP is

$$P_n = 1 - (1 - P_{A_c})^n \tag{5.10}$$

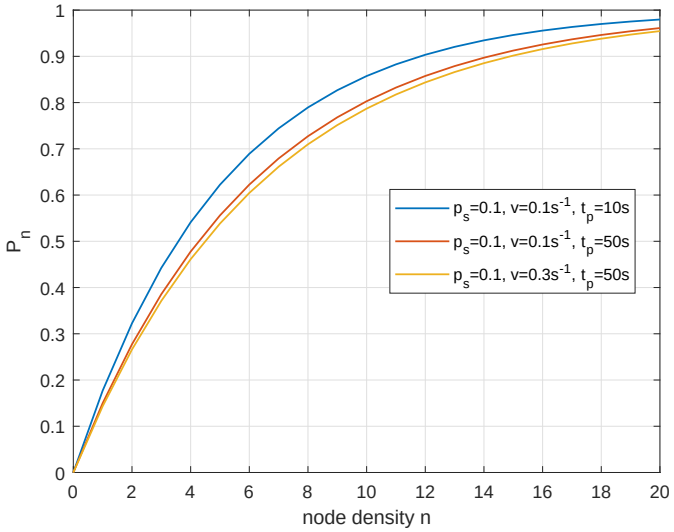

Figure 5.23: P_n under various parameters combinations

The probability P_n with various parameters combinations are shown in Figure 5.23. From the theoretical analysis results, with smaller v and t_p, a higher connected probability can be achieved. And with increasing node density n, the connected probability P_n also increases. Note that, with $p_s = 0.1$, $v = 0.1s^{-1}$ and $t_p = 10s$, when there are 6 nodes, the connected probability is almost 0.7. The disconnected period of CMP is not so long. To improve the CMP performance in an RWP environment, the cache routers and consumers should be connected during most of the network operational time. That is, when there is a link break due to the movement of the relay node, it is important for the system to find a replacement relay as soon as possible.

References

[1] OPNET Modeler. [Online]. Available: https://www.riverbed.com

[2] V. Jacobson, D. K. Smetters, J. D. Thornton, M. F. Plass, N. H. Briggs, and R. L. Braynard, "Networking named content," in Proc. 5th ACM CoNEXT, 2009.

[3] F. Jiang, Y. Sun and C. Phillips, "A Dual Sampling Cooperative Communication Method for Energy and Delay Reduction," 2018 IEEE 16th Intl Conf on Pervasive

Intelligence and Computing (PiCom), Athens, 2018, pp. 822-827.

[4] Feixiong Zhang, "Comparing alternative approaches for mobile content delivery in information-centric networking," 2015 IEEE 16th International Symposium on A World of Wireless, Mobile and Multimedia Networks (WoWMoM), Boston, MA, 2015, pp. 1-2.

[5] C. Bettstetter, G. Resta and P. Santi, "The node distribution of the random waypoint mobility model for wireless ad hoc networks," in IEEE Transactions on Mobile Computing, vol. 2, no. 3, pp. 257-269, July-Sept. 2003.

[6] Nour B, Sharif K, Li F, et al, "A survey of Internet of Things communication using ICN: A use case perspective," Computer Communications, 2019.

[7] Liu X, Li Z, Yang P, et al, "Information-centric mobile ad hoc networks and content routing: a survey," Ad Hoc Networks, 2017, 58: 255-268.

Chapter 6

UAV Trajectory Design

In this chapter, in order to improve the throughput of the UAV-aided wireless system, the simultaneous transmission technique named the DS method [1] is employed in the data transmission procedure. With the DS method enabled, the UAV is able to receive information of different ground terminals simultaneously rather than separating the transmission of each ground terminal within sequential time slots or by using different radio bands. Meanwhile, the UAV flight trajectory can be modified when the DS mechanism is enabled, which is different from the trajectory derived in [2] [3]. It is shown in [4] that the UAV flight trajectory is closely related to the UAV's propulsion energy. Hence different trajectories can result in different consumption of propulsion energy for the UAV.

The contributions of this chapter are listed as follows:

- Propose an iterative algorithm which alternately optimizes bandwidth scheduling and UAV flight trajectory in each iteration, and a power balancing method for supporting DS.
- Comparison of the system performance of a DS-enabled scheme and a non-DS scheme in terms of the optimal throughput, bandwidth scheduling and UAV tra-

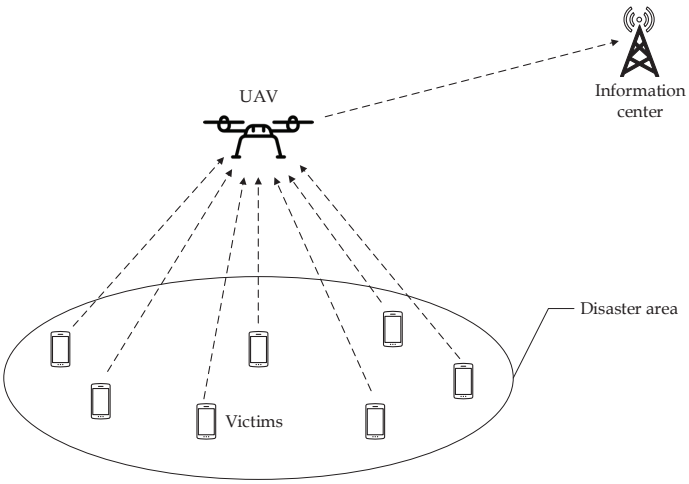

Figure 6.1: A UAV-aided wireless communication system in a disaster scenario

jectory.

- Comparison of the UAV propulsion energy consumption of a DS-enabled scheme and a non-DS scheme based on the derived optimal UAV trajectory.

It should be noted that the optimization takes place before the UAV is dispatched, acting as guidance for navigating the UAV flight path. The ground location of every ground terminal is important prior-knowledge for the system. And in the next section, the system model is presented.

6.1 System Model

The role of UAVs in the context of natural disaster management is identified in [5]. The main applications of systems involving UAVs are classified according to the disaster management phase, and a review of relevant research as well as the research challenges is provided in [5]. In this chapter, consider a disaster scenario where a UAV is deployed within the affected area to relay data from N ground victims to a remote information centre for coordinating search and rescue missions as the terrestrial infrastructure con-

necting the affected area and the information centre is damaged, as illustrated in Figure 6.1. The location of the nth victim is denoted by $\mathbf{c}_n \in \mathbb{R}^{2\times 1}$. The UAV is dispatched to collect data from the victims for a duration of T seconds. Assume that the UAV flies at a fixed altitude of H meters and denote its maximum speed as $V_{\max}$ in meters/second (m/s). The initial and final locations of the UAV are assumed to be pre-determined, whose horizontal coordinates are denoted as $\mathbf{c}_0$, $\mathbf{c}_F \in \mathbb{R}^{2\times 1}$, respectively. Assume that $||\mathbf{c}_F - \mathbf{c}_0|| \leq V_{\max}T$ such that there exists at least one feasible trajectory for the UAV to follow. For convenience, T is equally divided into K time slots, that is $T = K\delta_t$, where δ_t denotes the elemental slot length such that the UAV's location is considered unchanged by the ground victims during this time. Therefore, the UAV's trajectory can be approximated by the sequence $\{\mathbf{c}[k], k \in \{1, \ldots, K\}\}$, where $\mathbf{c}[k]$ denotes the UAV's location at time slot k. To be specific, $\mathbf{c}[K+1]$ corresponds to the final location of the UAV, i.e. $\mathbf{c}[K+1] = \mathbf{c}_F$.

I compare the data transmission performance of the system when the DS method is enabled or disabled. Assume the total bandwidth of the system and the maximum transmission power of each victim are the same. When DS is disabled, I consider two bandwidth allocation mechanisms. One is a fair allocation scheme [6], assuming N different sub-carriers with the same bandwidth W are fairly allocated to the N victims to avoid interference during the period T. The other is a bandwidth contention scheme [2] [3], assuming the overall bandwidth NW is occupied by one victim for data transmission during each time slot.

When DS is enabled, due to the limitations of transmission synchronisation and processing complexity, assume during each time slot only transmissions from one pair of victims can be supported. In order to ensure the proper functioning of the DS method, the signal level received by the UAV from the supported victims are kept the same [1]. Meanwhile, during each time slot, the non-DS supported victims are allocated a bandwidth W each. The supported victims can both transmit in the remaining bandwidth $NW - (N-2)W = 2W$ simultaneously [1]. Therefore, I denote the bandwidth schedul-

ing variable as $a_n[k] = 2$ if victim n is supported by DS at time slot k, and $a_n[k] = 1$ if victim n is not supported by DS, where $k \in \{1, \ldots, K\}$.

The following statements relate to the DS enabled scheme. The distance between the UAV and victim $n \in \{1, \ldots, N\}$ at time slot $k \in \{1, \ldots, K\}$ is given by

$$d_n[k] = \sqrt{||\mathbf{c}[k] - \mathbf{c}_n||^2 + H^2} \tag{6.1}$$

We use $P_n[k]$ to denote the transmission power of victim n at time slot k, and all victims have the same maximum transmission power $P_{\max}$. Furthermore, we assume that the channels from the victims to the UAV are dominated by LoS links. Thus, the channel power gain between victim n and the UAV in time slot k is given by

$$h_n[k] = \frac{\beta_0}{d_n^2[k]} = \frac{\beta_0}{||\mathbf{c}[k] - \mathbf{c}_n||^2 + H^2} \tag{6.2}$$

where β_0 represents the channel power gain at a reference distance of unit length. The data rate in bits/s/Hz for victim n at time slot k with respect to bandwidth W is given by[1]

$$R_n[k] = a_n[k] \log_2(1 + \frac{P_n[k]h_n[k]}{\sigma^2}) \tag{6.3}$$

where σ^2 is the power of the Additive White Gaussian Noise (AWGN) and the bandwidth W is equivalent to 1. Thus, the average data rate from victim n to the UAV is denoted as

[1]For the DS supported victims, the transmission bandwidth is $2W$. Since the noise power spectrum density is the same, the received noise power at the UAV is twice as that for a non-DS supported victim. However, the UAV treats the overlapping signal as the effective received signal [1], hence doubling the received signal power. As a result, the received SNR at the UAV for a DS supported victim is same as that for a non-DS supported victim.

$$R_n = \frac{1}{K}\sum_{k=1}^{K} R_n[k] \tag{6.4}$$

where the bandwidth scheduling variables set is $\mathcal{A} = \{a_n[k], \forall n, k\}$, the victim transmit power variables set is $\mathcal{P} = \{P_n[k], \forall n, k\}$, and the UAV's trajectory location variables set is $\mathcal{C} = \{\mathbf{c}[k], \forall k\}$.

6.2 Problem Formulation

For efficient transmission, whilst considering fairness among all the victims, the aim to maximize the minimum average data rate relayed by the UAV among all N victims. That is

$$\max_{\mathcal{A},\mathcal{P},\mathcal{C}} R \tag{6.5}$$

subject to

$$R_n \geq R, \ \forall n \tag{6.5a}$$

$$\sum_{n=1}^{N} a_n[k] \leq N + 2, \ \forall k \tag{6.5b}$$

$$a_n[k] \in \{1, 2\}, \ \forall n, k \tag{6.5c}$$

$$P_n[k] \leq P_{\max}, \ \forall n, k \tag{6.5d}$$

$$P_i[k]h_i[k] = P_j[k]h_j[k], \ \forall k, (a_i[k] = a_j[k] = 2, i \neq j) \tag{6.5e}$$

$$||\mathbf{c}[k+1] - \mathbf{c}[k]|| \leq V_{\max}\delta_t, \ \forall k \in \{1, \ldots, K\} \tag{6.5f}$$

$$\mathbf{c}[1] = \mathbf{c}_0, \ \mathbf{c}[K+1] = \mathbf{c}_F \tag{6.5g}$$

where (6.5a) represents the max-min objective function. (6.5b) assumes that one pair of victims can be supported by the DS method during each time slot. (6.5c) considers that a victim can be either supported by the DS method or not. Equations (6.5d) and (6.5e) define the constraints of transmission power during each time slot, especially for the DS method supported victims, whose received signal power at the UAV should be the same. (6.5f) means that the maximum traverse distance of the UAV is limited by its maximum flying speed during each time slot. In addition, (6.5g) shows the predetermined initial and final locations of the UAV trajectory.

6.3 Proposed Solution

UAV communications usually involve the joint optimization of UAV trajectory and communication resource allocation. The more general optimization framework is with Block Coordinate Descent (BCD) and Successive Convex Approximation (SCA) techniques. To deal with the nonconvexity problem, BCD can be used to alternately update the communication resource allocation and UAV trajectory [10]. To be concretely in this section, I propose an iterative algorithm for solving the optimization problem (6.5) subject to constraints (6.5a)-(6.5g). The overall problem is separated into two sub-problems. To be specific, for a given UAV trajectory $\mathcal{C}$, we optimize the victim bandwidth scheduling $\mathcal{A}$ by solving a linear programming formulation. On the other hand, for any given victim bandwidth scheduling $\mathcal{A}$, the UAV trajectory $\mathcal{C}$ is optimized based on solving a quadratically constrained quadratic programming problem. Furthermore, to ensure the best decoding performance of the DS method by the UAV, the received signal power from the paired victims should be the same [1]. Along with this, power balancing is implemented to link the two sub-problems. Finally, we present the overall algorithm as a combination of the two sub-problems and power balancing.

6.3.1 Victim Bandwidth Scheduling Optimization

For any given UAV trajectory $\mathcal{C}$, problem (6.5) is simplified as[2]

$$\max_{\mathcal{A}} R \tag{6.6}$$

subject to

$$R_n \geq R, \ \forall n \tag{6.6a}$$

$$\sum_{n=1}^{N} a_n[k] \leq N + 2, \ \forall k \tag{6.6b}$$

$$a_n[k] \in \{1, 2\}, \ \forall n, k \tag{6.6c}$$

Sub-problem (6.6) is hard to solve as the optimization variable $\mathcal{A}$ involves integers. To solve this sub-problem, we first relax the integer variable restriction in (6.6c), allowing for continuous variables, which results in the following sub-problem

$$\max_{\mathcal{A}} R \tag{6.7}$$

subject to

$$R_n \geq R, \ \forall n \tag{6.7a}$$

$$\sum_{n=1}^{N} a_n[k] \leq N + 2, \ \forall k \tag{6.7b}$$

$$1 \leq a_n[k] \leq 2, \ \forall n, k \tag{6.7c}$$

[2]In this sub-problem, the bandwidth scheduling $\mathcal{A}$ is to be determined, thus which victims are supported by the DS method in each time slot at this stage are not known.

The sub-problem (6.7) is a standard linear programming problem, which can be solved by the CVX toolbox [7] in MATLAB. Later in the description of the overall algorithm, we explain how to construct a solution for problem (6.5) based on sub-problem (6.7).

6.3.2 UAV Trajectory Optimization

For any given victim bandwidth scheduling $\mathcal{A}$, problem (6.5) is simplified as

$$\max_{\mathcal{C}} R \tag{6.8}$$

subject to

$$R_n \geq R, \ \forall n \tag{6.8a}$$

$$||\mathbf{c}[k+1] - \mathbf{c}[k]|| \leq V_{\max}\delta_t, \ \forall k \in \{1, \ldots, K\} \tag{6.8b}$$

$$\mathbf{c}[1] = \mathbf{c}_0, \ \mathbf{c}[K+1] = \mathbf{c}_F \tag{6.8c}$$

The constraint (6.8a) is equivalent to the following expression

$$\frac{1}{K}\sum_{k=1}^{K} a_n[k] \log_2(1 + \frac{P_n[k]\gamma_0}{||\mathbf{c}[k] - \mathbf{c}_n||^2 + H^2}) \geq R, \ \forall n$$

where $\gamma_0 \triangleq \frac{\beta_0}{\sigma^2}$. Note that (6.8a) is a non-convex constraint regarding the UAV trajectory variable $\mathbf{c}[k]$. To deal with it, the expression in (6.8a) is replaced by its lower bound at a given local point. We denote the input UAV trajectory for sub-problem (6.7) as $\{\mathbf{c}'[k], k \in \{1, \ldots, K\}\}$. Recalling that the logarithmic function is lower bounded by its first order Taylor expansion, we can obtain the following lower bound with the given local point $\mathbf{c}'[k]$ when treating $||\mathbf{c}[k] - \mathbf{c}_n||^2$ as the variable

$$
\begin{aligned}
R_n[k] &= a_n[k]\log_2(1+\frac{P_n[k]\gamma_0}{||\mathbf{c}[k]-\mathbf{c}_n||^2+H^2}) \\
&\geq a_n[k]\left[A_n[k](||\mathbf{c}[k]-\mathbf{c}_n||^2-||\mathbf{c}'[k]-\mathbf{c}_n||^2)+B_n[k]\right] \triangleq R_n^{lb}[k]
\end{aligned}
\tag{6.9}
$$

where

$$
A_n[k] = \frac{-P_n[k]\gamma_0\log_2 e}{(||\mathbf{c}'[k]-\mathbf{c}_n||^2+H^2)(||\mathbf{c}'[k]-\mathbf{c}_n||^2+H^2+P_n[k]\gamma_0)} \tag{6.9a}
$$

$$
B_n[k] = \log_2(1+\frac{P_n[k]\gamma_0}{||\mathbf{c}'[k]-\mathbf{c}_n||^2+H^2}),\ \forall n,k \tag{6.9b}
$$

With the lower bound (6.9), sub-problem (6.8) is approximated as the following sub-problem

$$
\max_{\mathcal{C}} R^{lb} \tag{6.10}
$$

subject to

$$
R_n^{lb} = \frac{1}{K}\sum_{k=1}^{K} R_n^{lb}[k] \geq R^{lb},\ \forall n \tag{6.10a}
$$

$$
||\mathbf{c}[k+1]-\mathbf{c}[k]|| \leq V_{\max}\delta_t,\ \forall k \in \{1,\ldots,K\} \tag{6.10b}
$$

$$
\mathbf{c}[1]=\mathbf{c}_0,\ \mathbf{c}[K+1]=\mathbf{c}_F \tag{6.10c}
$$

For (6.10a) the victim bandwidth scheduling variable $a_n[k]$ is determined by solving the sub-problem (6.7) and the victim transmission power variable $P_n[k]$ is determined by implementing the power balancing mechanism. Hence both (6.10a) and (6.10b) are convex quadratic constraints and (6.10c) is a linear constraint. Therefore, sub-problem

(6.10) is a convex quadratically constrained quadratic program which can be solved efficiently by the MATLAB CVX toolbox [7].

6.3.3 Power Balancing

A power balancing mechanism is implemented to ensure the signal power received at the UAV from the DS supported victims are the same during each time slot. Upon solving sub-problem (6.7), the victim bandwidth scheduling variable is determined.

Within each time slot, for DS method supported victims, the corresponding received signal powers should be the same. As the maximum transmission power for the paired victims are both $P_{\max}$, therefore when the UAV locates at a position where its distances to the paired victims are same, the optimal max-min data rate for both victims can be achieved. Hence, the corresponding UAV's position should be the result that is achieved by solving sub-problem (6.10). In order to obtain the ideal UAV's position, the coefficients $A_n[k]$ and $B_n[k]$ in constraint (6.10a) should be pre-adjusted to be the same. The expected UAV's position can then be calculated as the shortest same distance to both paired victims in sub-problem (6.10) resulting in optimal max-min data rate which satisfies the objective function. Power balancing is the operation of coefficient pre-adjustment, which is implemented to connect sub-problems (6.7) and (6.10).

6.3.4 Overall Algorithm

Based on the results of the two sub-problems (6.7) and (6.10), we propose an overall iterative algorithm for problem (6.5). Specifically, during each iteration, the victim bandwidth scheduling $\mathcal{A}$ and UAV flight trajectory $\mathcal{C}$ are alternately optimized, by solving each sub-problem (6.7) or (6.10) in turn whilst maintaining the other variables unchanged. Moreover, the solution achieved in each iteration is used as the input to the next iteration. Details of the algorithm are provided in Algorithm 1. As stated, power

balancing is implemented to connect the two sub-problems. Furthermore, at the end of the algorithm, we construct the optimal integer victim bandwidth scheduling from the continuous values calculated by the iterative approach.

Algorithm 1 Iterative solution for problem (6.5)

1: Initialize the UAV trajectory, and denote it as $\mathcal{C}^0$.
2: Denote the iteration number variable as g, and let $g = 0$.
3: **repeat**
4: Solve sub-problem (6.7) for given $\mathcal{C}^g$, and denote the optimal solution as $\mathcal{A}^{g+1}$.
5: Perform power balancing.
6: Solve sub-problem (6.10) for given $\mathcal{A}^{g+1}$, $\mathcal{C}^g$, and denote the optimal solution as $\mathcal{C}^{g+1}$.
7: Update $g = g + 1$.
8: **until** The increase of the objective value is below a threshold th.
9: Treat the optimal solution $\mathcal{C}^{g+1}$ for the last iteration as the optimal UAV trajectory.
10: Construct the optimal victim bandwidth scheduling based on the optimal solution $\mathcal{A}^{g+1}$ for the last iteration.

In the solution obtained by Algorithm 1, if the victim bandwidth scheduling variables $a_n[k]$ are all integer, then the obtained solution is a feasible solution of problem (6.5). Otherwise, for all the non-integer $a_n[k]$, the range for the value should be $1 < a_n[k] < 2$. We denote the fractional part as $b_n[k] = a_n[k]-1$. During each time slot δ_t, we can regard that the expectation of the victim bandwidth scheduling as $a_n[k]$. Thus, for a specific victim with given $a_n[k]$, in the period of $\delta_t b_n[k]$ the bandwidth scheduling is configured as 2, and in the remaining period $\delta_t(1 - b_n[k])$, the bandwidth scheduling is configured as 1. Therefore, the integer victim bandwidth scheduling is constructed based on the non-integer value.

Next, we consider the convergence of Algorithm 1 as follows. First we define the objective variable R as a function of $\mathcal{A}$ and $\mathcal{C}$; that is $R = \eta(\mathcal{A}, \mathcal{C})$. In step 4 of Algorithm 1, since the optimal solution of sub-problem (6.7) is obtained for a given $\mathcal{C}^g$, then

$$\eta(\mathcal{A}^g, \mathcal{C}^g) \leq \eta(\mathcal{A}^{g+1}, \mathcal{C}^g) \tag{6.11}$$

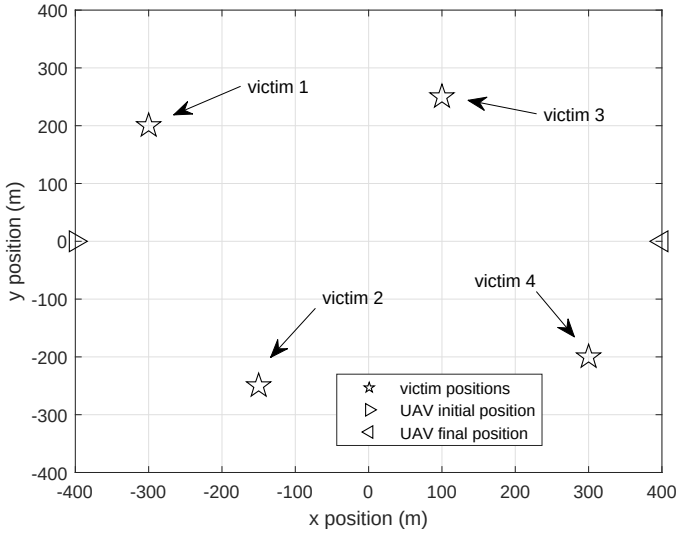

Figure 6.2: A disaster scenario topology

Then for given $\mathcal{A}^{g+1}$ and $\mathcal{C}^{g}$ in step 6 of Algorithm 1, it follows that

$$\eta(\mathcal{A}^{g+1}, \mathcal{C}^{g}) \leq \eta^{lb,g}(\mathcal{A}^{g+1}, \mathcal{C}^{g+1}) \tag{6.12a}$$

$$\eta^{lb,g}(\mathcal{A}^{g+1}, \mathcal{C}^{g+1}) \leq \eta(\mathcal{A}^{g+1}, \mathcal{C}^{g+1}) \tag{6.12b}$$

where (6.12a) holds since $\eta(\mathcal{A}^{g+1}, \mathcal{C}^{g})$ has the same objective value as $\eta^{lb,g}(\mathcal{A}^{g+1}, \mathcal{C}^{g})$ at the given point $\mathcal{C}^{g}$, and $\eta^{lb,g}(\mathcal{A}^{g+1}, \mathcal{C}^{g}) \leq \eta^{lb,g}(\mathcal{A}^{g+1}, \mathcal{C}^{g+1})$ since at Step 6 of Algorithm 1 with given $\mathcal{A}^{g+1}$, sub-problem (6.10) is solved optimally with solution $\mathcal{C}^{g+1}$. (6.12b) holds because for any iteration g, $\eta^{lb,g}(\mathcal{A}^{g}, \mathcal{C}^{g})$ is always a lower bound of $\eta(\mathcal{A}^{g}, \mathcal{C}^{g})$ for any $\mathcal{A}$ and $\mathcal{C}$. Based on (6.11), (6.12a) and (6.12b), obtain $\eta(\mathcal{A}^{g}, \mathcal{C}^{g}) \leq \eta(\mathcal{A}^{g+1}, \mathcal{C}^{g+1})$, which means that the objective value of problem (6.5) is non-decreasing after each iteration of Algorithm 1. As the objective value of problem (6.5) is upper bounded by a finite value, Algorithm 1 is therefore convergent.

Table 6-A: Comparison of optimal max-min throughput (bits/s/Hz)

	$T = 60$s	$T = 40$s	$T = 30$s	$T = 20$s
non-DS bandwidth contention scheme	10.40	9.99	9.63	9.12
non-DS fair bandwidth allocation scheme	9.80	9.78	9.76	9.71
DS method	14.65	14.64	14.62	14.58

6.4 Numerical Results

In this chapter, the main metric to assess the system is the throughput among all the victims which is expressed in units of bits/s/Hz. With a higher throughput, on average more data can be transmitted to the UAV from the victims. Additionally, the victim bandwidth scheduling and the UAV optimal flight trajectory are also metrics for evaluating the system performance.

Consider a system with $N = 4$ victims that are located within an area of size 800×800 m^2 as illustrated in Figure 6.2. The UAV is assumed to fly at a fixed altitude of $H = 100$ m. The receiver noise power is assumed to be $\sigma^2 = -110$ dBm. The channel power gain at the reference distance of unit length is set to $\beta_0 = -50$ dB. The maximum transmit power for the victim is set to $P_{\max} = 0.1$ W and the maximum flight speed of the UAV is set to $V_{\max} = 50$ m/s. The total number of time slots is assumed to be $K = 20$. The threshold to control the iteration of the solution algorithm is set as $th = 10^{-2}$.

In this section, we compare the DS enabled scheme with the non-DS schemes, which comprise a fair bandwidth allocation and a bandwidth contention mechanism. First we list the optimal max-min throughput for the different schemes for various total period values T in Table 6-A. Figure 6.3 shows the optimal UAV flight trajectories for the different schemes when $T = 60$s. The DS method has the best performance in terms of throughput, since the bandwidth is multiplexed by a pair of victims in each time slot. The non-DS bandwidth contention scheme has better throughput performance than the non-DS fair bandwidth allocation scheme as the UAV flies to and hovers above each victim in the bandwidth contention scheme, which brings better channel gain for data transmission.

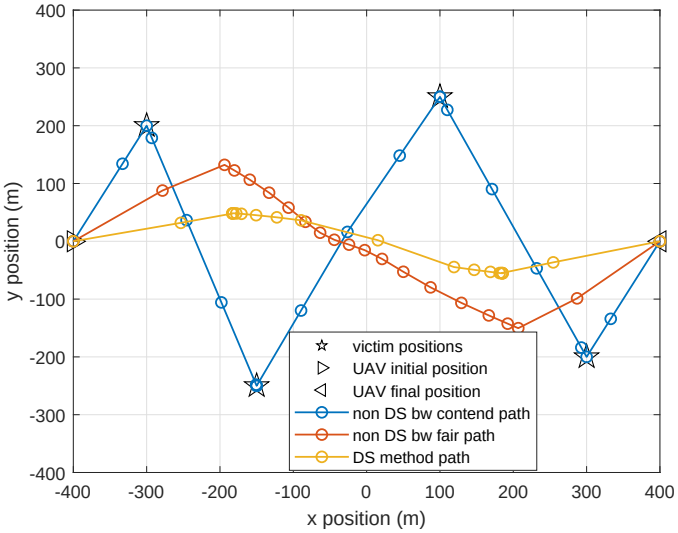

Figure 6.3: Comparison of optimal max-min throughput UAV trajectories - $T = 60$s

Figure 6.4 and Figure 6.5 show the bandwidth scheduling for each victim in the DS method and non-DS bandwidth contention scheme, respectively. In the DS scheme, victim 1 and victim 2 are supported by the DS method first, then victim 3 and victim 4 are supported by the DS method. However, in the non-DS bandwidth contention scheme, from victim 1 to victim 4, each of them occupies the bandwidth sequentially. The bandwidth scheduling configurations are delivered to the victims by the UAV via control signals.

Figure 6.6 shows the optimal trajectories for the non-DS bandwidth contention scheme for different T values. As the period T decreases, the maximum distance that the UAV can traverse between the initial and final positions decreases, thus the UAV flight trajectory eventually becomes unable to reach every victim. However, the UAV tries to approach each victim as close as possible. Meanwhile, the channel gain worsens as the distance between the UAV and victim is increasing, hence resulting in a decrease of the optimal max-min throughput.

Figure 6.7 shows the optimal trajectories for the non-DS fair bandwidth allocation scheme for different T values. The optimal throughput for the non-DS fair bandwidth

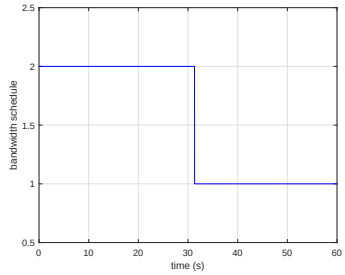

(a) victim 1 bandwidth schedule

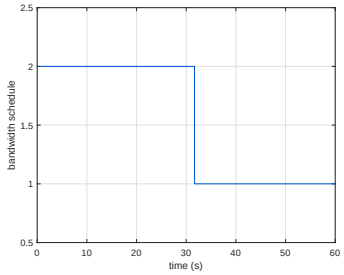

(b) victim 2 bandwidth schedule

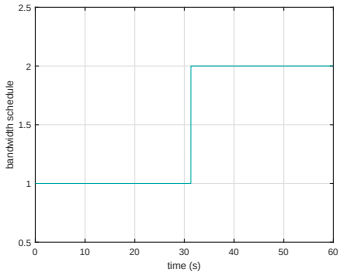

(c) victim 3 bandwidth schedule

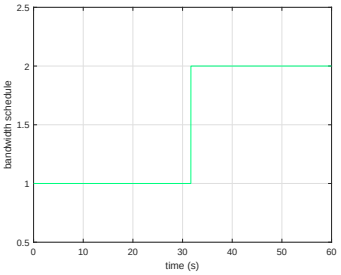

(d) victim 4 bandwidth schedule

Figure 6.4: DS method bandwidth schedule - $T = 60$s

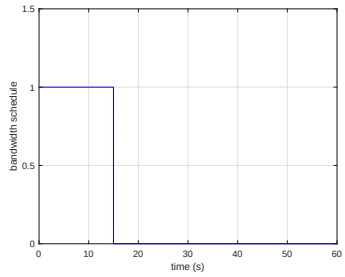

(a) victim 1 bandwidth schedule

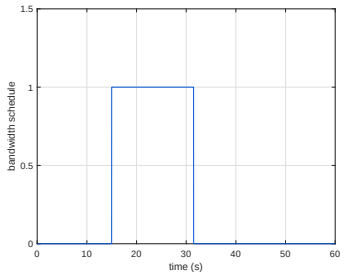

(b) victim 2 bandwidth schedule

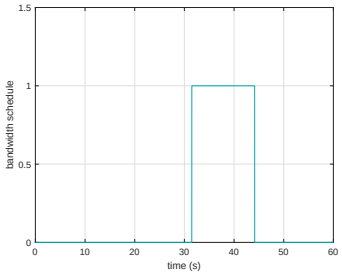

(c) victim 3 bandwidth schedule

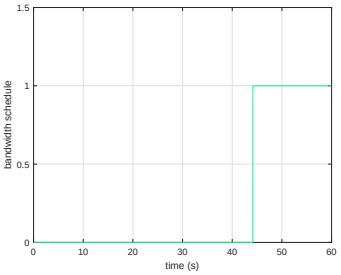

(d) victim 4 bandwidth schedule

Figure 6.5: Non-DS method bandwidth contention schedule - $T = 60$s

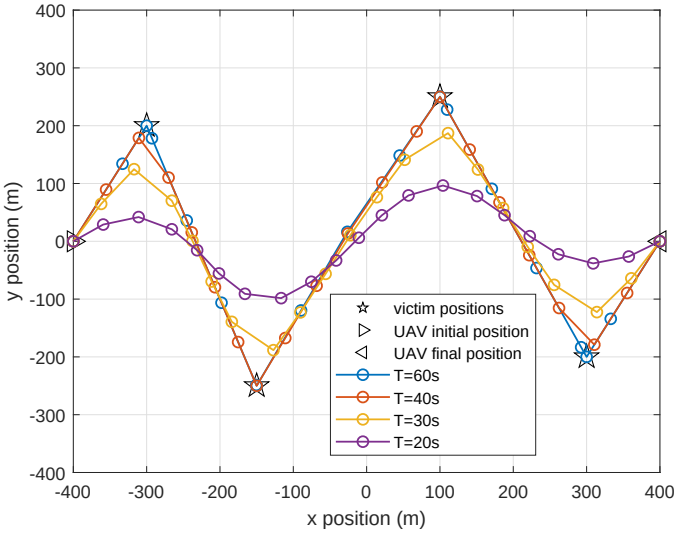

Figure 6.6: Non-DS bandwidth contention scheme optimal UAV trajectory comparison

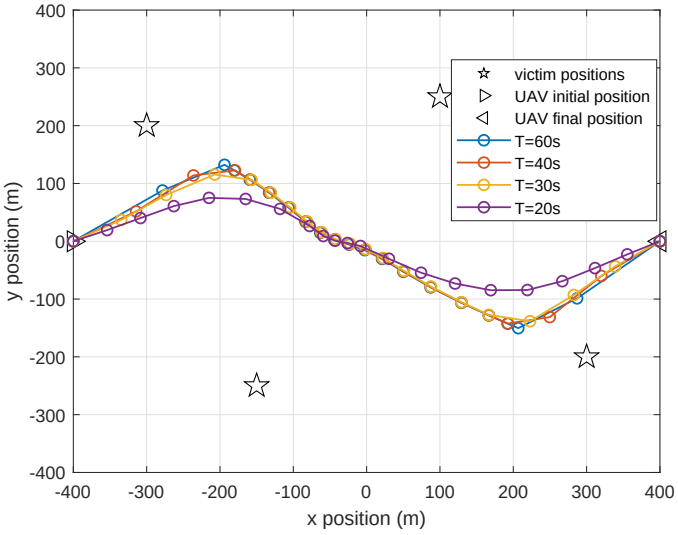

Figure 6.7: Non-DS fair bandwidth scheme optimal UAV trajectory comparison

allocation scheme decreases slightly as the period T decreases. This is because in the non-DS fair bandwidth allocation scheme, the UAV flies along a trajectory where the distances from each victim to the UAV do not vary much. The length of the trajectory is covered by the maximum UAV traversal distance for different T. Therefore the change of T slightly changes the optimal UAV flight trajectory.

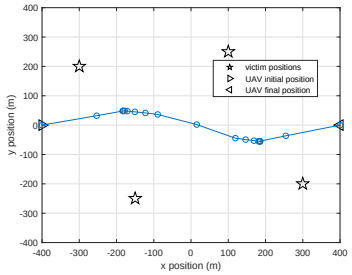

(a) optimal trajectory - $T = 60$s

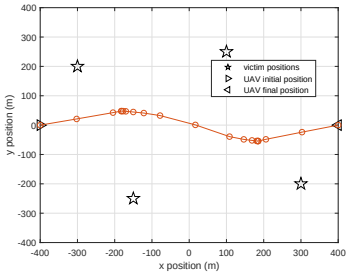

(b) optimal trajectory - $T = 40$s

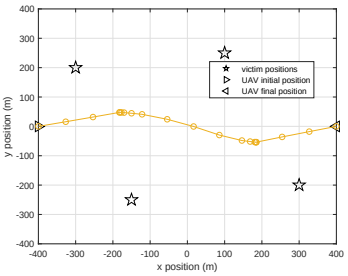

(c) optimal trajectory - $T = 30$s

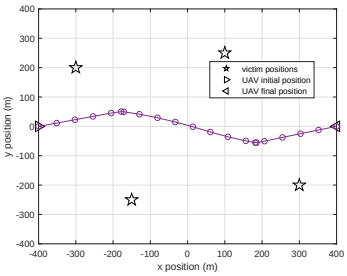

(d) optimal trajectory - $T = 20$s

Figure 6.8: DS method optimal trajectories comparison

Figure 6.8 shows the optimal trajectories for the DS method for different T values. The change of the period T only changes the optimal throughput slightly. In the DS method, the UAV is likely to fly to positions that are the same distance from both of the DS supported paired victims. Hence the change of T only slightly affects the UAV flight trajectory.

Next, we compare the propulsion energy consumed by the UAV for different schemes. As derived in [8], the propulsion power consumption for a rotary-wing UAV in a time slot can be modelled as

$$P[k] = P_0(1 + \frac{3v[k]^2}{U_{\text{tip}}^2}) + P_i(\sqrt{1 + \frac{v[k]^4}{4v_0^4}} - \frac{v[k]^2}{2v_0^2})^{1/2} + \frac{1}{2}d_0\rho sAv[k]^3 \tag{6.13}$$

where $v[k]$ is the constant flight speed of the UAV in a time slot. P_0 and P_i represent the blade profile power and induced power in hovering status, respectively. U_{tip} denotes the tip speed of the rotor blade, v_0 is known as the mean rotor induced velocity

Table 6-B: UAV propulsion energy (kJ) comparison

	$T = 60$s	$T = 40$s	$T = 30$s	$T = 20$s
non-DS bandwidth contention scheme	88.43	63.83	51.21	34.14
non-DS fair bandwidth allocation scheme	69.77	45.26	36.26	30.84
DS method	76.83	69.78	62.24	52.24

in hover, and d_0 and s are the fuselage drag ratio and rotor solidity, respectively. ρ and A denote the air density and rotor disc area, respectively. Therefore, the propulsion energy in a time slot is $P[k]\delta_t$. Furthermore, the overall propulsion energy of the UAV is

$$E = \sum_{k=1}^{K} P[k]\delta_t \tag{6.14}$$

Assume that $P_0 = 577.3$W, $P_i = 793.0$W, $U_{\text{tip}} = 200$m/s, $v_0 = 7.21$m/s, $d_0 = 0.3$, $\rho = 1.225$kg/m^3, $s = 0.05$, and $A = 0.79$m^2 [9]. Based on the optimal UAV trajectory derived for different schemes, the overall propulsion energy consumed by the UAV is listed in Table 6-B. On observing the results, for shorter time periods, that is when $T = 40$s, 30s, and $20s$, the DS method consumes most propulsion energy, while the non-DS fair bandwidth allocation scheme consumes the least propulsion energy. In the DS method, the UAV hovers for the longest time, and in the two non-DS schemes, it hovers for much less time. When the UAV flight speed is less than around 40m/s, it consumes most power; this is worst when it remains in the hovering state [9]. This is why the UAV consumes most propulsion energy in the DS method. However, for a longer time period, when $T = 60$s, the non-DS bandwidth contention scheme consumes the most propulsion energy. This is because the UAV hovers at the position of each victim during the whole procedure. The DS method consumes more energy than the non-DS fair bandwidth allocation scheme, but it achieves higher max-min throughput among all the victims.

6.5 UAV Trajectory Design Conclusions

In this chapter, we have considered the DS method simultaneous transmission technique in regard to the UAV flight trajectory, so as to maximize the minimum data transmission throughput among all the victims. In order to solve the problem, we propose an iterative algorithm which alternately optimizes the victim bandwidth scheduling and UAV trajectory. In addition, power balancing is implemented in each iteration of the algorithm for supporting the DS method. Comparing the DS scheme with two non-DS schemes, i.e. a fair bandwidth allocation scheme and a bandwidth contention scheme, the DS scheme outperforms the non-DS schemes in terms of the optimal max-min throughput among all the victims. The optimal UAV flight trajectory for the DS scheme is different from the non-DS bandwidth contention scheme and non-DS fair bandwidth allocation scheme, as the UAV flies to positions that are not particularly close to each victim. For the UAV propulsion energy consumption, for shorter time periods, the non-DS fair bandwidth allocation scheme consumes the least energy. For longer time periods, the DS method consumes the second least energy but with the highest max-min throughput among all victims.

References

[1] F. Jiang, Y. Sun and C. Phillips, "A Dual Sampling Cooperative Communication Method for Energy and Delay Reduction," 2018 IEEE 16th Intl Conf on Pervasive Intelligence and Computing (PiCom), Athens, 2018, pp. 822-827.

[2] C. Zhan, Y. Zeng and R. Zhang, "Energy-Efficient Data Collection in UAV Enabled Wireless Sensor Network," in IEEE Wireless Communications Letters, vol. 7, no. 3, pp. 328-331, June 2018.

[3] Q. Wu, Y. Zeng and R. Zhang, "Joint Trajectory and Communication Design for UAV-Enabled Multiple Access," GLOBECOM 2017 - 2017 IEEE Global Communications Conference, Singapore, 2017, pp. 1-6.

[4] D. Yang, Q. Wu, Y. Zeng and R. Zhang, "Energy Tradeoff in Groundto-UAV Communication via Trajectory Design," in IEEE Transactions on Vehicular Technology, vol. 67, no. 7, pp. 6721-6726, July 2018.

[5] Milan Erdelj, Micha Krl, Enrico Natalizio, "Wireless Sensor Networks and Multi-UAV systems for natural disaster management," Computer Networks, Volume 124, Pages 72-86, 2017.

[6] Y. Cai, Z. Wei, R. Li, D. Ng and J. Yuan. "Energy-Efficient Resource Allocation for Secure UAV Communication Systems," in IEEE WCNC Proceedings, 2019.

[7] http://cvxr.com/cvx/

[8] Y. Zeng, J. Xu and R. Zhang, "Energy Minimization for Wireless Communication With Rotary-Wing UAV," in IEEE Transactions on Wireless Communications, vol. 18, no. 4, pp. 2329-2345, April 2019.

[9] Y. Zeng, J. Xu and R. Zhang, "Rotary-Wing UAV Enabled Wireless Network: Trajectory Design and Resource Allocation," 2018 IEEE Global Communications Conference (GLOBECOM), Abu Dhabi, United Arab Emirates, 2018, pp. 1-6.

[10] Zeng Y, Wu Q, Zhang R. "Accessing from the sky: A tutorial on UAV communications for 5G and beyond," Proceedings of the IEEE, 2019, 107(12): 2327-2375.

Chapter 7

Conclusions

In this research, a DS method is proposed. Firstly, reducing the transmission phases in two-way three-terminal communications with the DS method is explained. The information contained within the even-sampling instants is the main factor that affects the performance of the DS scheme. Simulation results show that the DS method performs effectively at the relay node. Secondly, the BER expressions for both DF relaying and DS cooperative communication in a one-way transmission three-terminal scenario are derived. The derivations reveal the potential energy efficiency of DS cooperative communication over DF. Finally, an expression for estimating the number of cooperative clusters in a wireless network is presented. Additional simulations reveal the energy saving and delay reduction benefits of the proposed DS cooperative communication method.

Coded caching is a promising paradigm which exploits coding multiple transmissions, providing a global transmission gain. In this research, a CMP for coded caching networks to support the DS method during the content delivery stage between the cache routers and consumers is proposed. I demonstrate the design of the proposed protocol, including the packet flow handling and the scheme's implementation on OPNET. Then I compare CMP-DS against traditional NDN content delivery in terms of the

number of transmissions, the average end-to-end delay and the average throughput. As CMP manages to select appropriate nodes for cache migration, the DS method is supported seamlessly. With fewer transmission phases, CMP-DS outperforms the traditional NDN method. It also shows that CMP is able to re-select nodes for cache migration when a consumer moves. CMP provides an effective approach for exploiting simultaneous transmissions to achieve extra performance gains, especially in terms of reduced transmission latency.

Finally, in this research I consider the DS simultaneous transmission technique in regard to UAV flight trajectory planning, so as to maximize the minimum data transmission throughput among all the victims. In order to solve the problem, I propose an iterative algorithm which alternately optimizes the victim bandwidth scheduling and UAV trajectory. In addition, power balancing is implemented in each iteration of the algorithm for supporting the DS method. Then I compare the DS scheme with two non-DS schemes, i.e. a fair bandwidth allocation scheme and a bandwidth contention scheme. The DS scheme outperforms the non-DS schemes in terms of the optimal max-min throughput among all the victims. The optimal UAV flight trajectory for the DS scheme is different from the non-DS bandwidth contention scheme and non-DS fair bandwidth allocation scheme, where the UAV flies to positions that are not relatively close to each victim. In terms of UAV propulsion energy consumption, for shorter time periods, the non-DS fair bandwidth allocation scheme consumes the least energy. For longer time periods, the DS method consumes the second least energy but with highest max-min throughput among all the victims.

Based on the above statements, the DS method can be regarded as an optional promising transmission mechanism when multiple users transmit simultaneously, characterised by a large increase in the amount of users and data traffic. However, specific design factors should be considered to fully exploit the advantages that the DS method can bring to the given application scenario. Finally, I would like to talk about some future directions regarding this research. For the DS method, more than two simultane-

ous transmissions could be considered thus extending its applicability but this would involve a more complex theoretical design. For the UAV-aided wireless network, scenarios where more than one UAV are deployed could be explored.

Appendix A

Author's publications

1. **F. Jiang**, Y. Sun and C. Phillips, "A Dual Sampling Cooperative Communication Method for Energy and Delay Reduction," *2018 IEEE 16th Intl Conf on Pervasive Intelligence and Computing (PiCom)*, Athens, 2018, pp. 822-827. (Published)

2. **F. Jiang**, Y. Sun and C. Phillips, "Cache Migration Protocol for Information-Centric Networks," *2019 IEEE Wireless Communications and Networking Conference Workshop (WCNCW)*, Marrakech, Morocco, 2019, pp. 1-6. (Published)